

Exploring the Naturalness of AI-Generated Images

Zijian Chen¹, Wei Sun^{1*}, Haoning Wu², Zicheng Zhang¹,
Jun Jia¹, Xiongkuo Min¹, Guangtao Zhai^{1*}, Wenjun Zhang¹
¹Shanghai Jiao Tong University ²Nanyang Technological University
*Corresponding author

Abstract

The proliferation of Artificial Intelligence-Generated Images (AGIs) has greatly expanded the Image Naturalness Assessment (INA) problem. Different from early definitions that mainly focus on tone-mapped images with limited distortions (e.g., exposure, contrast, and color reproduction), INA on AI-generated images is especially challenging as it has more diverse contents and could be affected by factors from multiple perspectives, including low-level technical distortions and high-level rationality distortions. In this paper, we take the first step to benchmark and assess the visual naturalness of AI-generated images. First, we construct the *AI-Generated Image Naturalness (AGIN)* database by conducting a large-scale subjective study to collect human opinions on the overall naturalness as well as perceptions from technical and rationality perspectives. AGIN verifies that naturalness is universally and disparately affected by both technical and rationality distortions. Second, we propose the *Joint Objective Image Naturalness evaluator (JOINT)*, to automatically learn the naturalness of AGIs that aligns human ratings. Specifically, JOINT imitates human reasoning in naturalness evaluation by jointly learning both technical and rationality perspectives. Experimental results show our proposed JOINT significantly surpasses baselines for providing more subjectively consistent results on naturalness assessment. Our database and code will be released in <https://github.com/zijianchen98/AGIN>.

1. Introduction

Recent advancements in deep generative models have sparked a new craze in Artificial Intelligence-Generated Images (AGIs), which have gained significant progress across various applications, including text-to-image generation [19, 62, 66, 73, 74, 76], image translation [34, 41, 70, 99, 104], image inpainting [51, 60], image colorization [35, 83, 92], and image editing [6, 69, 100]. However, even cutting-edge models occasionally generate irrational content or technical

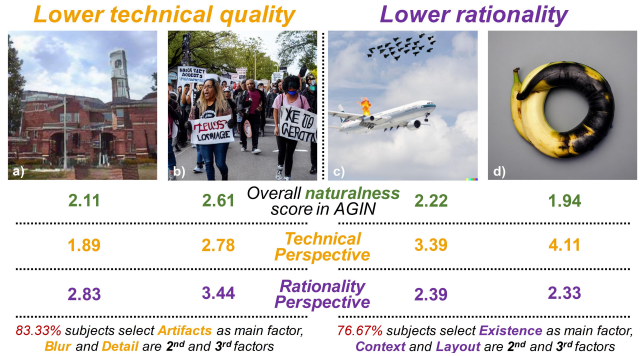


Figure 1. **Exemplar images with diverged technical quality and rationality.** Evaluating image naturalness from different perspectives (*technical/rationality*) may produces biases, motivating us to construct AGIN, the first INA database with opinions from multi-perspectives.

artifacts in the image, which we refer to as the image naturalness problem. Unlike natural scene images (NSIs) that are captured from real-world scenes, AI-driven image generation harnesses neural networks to learn synthesis rules from extensive image datasets [9, 59, 91]. Its instability and randomness of generation mode attach AGIs with more diverse content, leading to varying degrees of naturalness, which often requires retouching and filtering before practical use so as to avoid misleading people and negative social repercussions. Consequently, objective models for evaluating the naturalness of AGIs are urgently needed.

Conventionally, image naturalness is described as the degree of correspondence between a real-life scene and a photograph displayed on a device based on some technical criteria (e.g., texture, exposure, color reproduction, shooting artifacts) [8, 14, 18], which has been utilized for image quality assessment (IQA) to compare and guide the optimization of systems and algorithms [24, 44, 93]. Under this perspective, the image with richer details (Fig. 1c, Fig. 1d) should have notably better naturalness than blur image in Fig. 1a. More recently, the emergence of AGI broadens the definition of image naturalness to comprise more non-technical semantic factors (e.g., existence, layout), which is normally regarded as the rationality perspective [45, 59]. However, it

is highly subjective and its mechanism of how rationality affects human perception in image naturalness reasoning, *i.e.*, *human-naturalness opinions*, is still ambiguous and may be multidimensionally coupled.

In this paper, we make the first attempt to evaluate naturalness of AI-generated images, a new field of quality assessment with increasing attention [12, 50, 68, 91, 109]. To benchmark naturalness of AI-generated images, we contribute AI-Generated Image Naturalness (AGIN) database, the first-of-its-kind database to study this problem. Specifically, AGIN contains 6,049 images collected from five different generative tasks with 18 model variants to ensure diversity. A total of 907,350 human opinions for technical and rationality perspectives as well as their effects on overall naturalness scores were collected from 30 participants. Since the perspectives and factors studied in our research are related to common IQA problems and not limited to AI-generated images, our methods and insights also can be applicable to other forms of multimedia.

AGIN provides several valuable observations for understanding human reasoning in visual naturalness. Firstly, we find both technical distortions (*e.g.*, *contrast*, *blur*, and *generative artifacts*) and rationality distortions (*e.g.*, *existence*, *color*, and *layout*) can affect visual naturalness significantly. The proportion of technical and rationality factors for AGIs with worse naturalness scores ($MOS \in [1, 3]$) is about 1:1.17. Secondly, we notice that most factors in the two perspectives are relevant, but have disparate impacts on the naturalness score, which can result in biased naturalness assessment. Furthermore, we also observe that the overall naturalness score can be well-approximated by a linear weighted sum of technical score and rationality score ($MOS = 0.145MOS_T + 0.769MOS_R$). This correlation suggests joint learning of technical and rationality branches can be a feasible way to model naturalness.

Based on AGIN database, we propose the Joint Objective Image Naturalness evaluator (JOINT), an objective naturalness assessment method that offers high alignment with human perception. JOINT aims to mimic human reasoning of image naturalness by jointly learning on both technical and rationality branches. Specifically, given the different characteristics of each branch, we elaborate several designs, such as *patch partition*, *deep feature regularization*, and *pretraining*, to allocate each branch with corresponding learning interests. Two different supervision schemes including using the overall naturalness scores (JOINT) and the respective scores for each perspective (JOINT++), are applied to train the model. Finally, we use an effective subjective weighting strategy combined with the predictions of two branches to compute the overall naturalness score. Experimental results on AGIN database verify the effectiveness of our proposed JOINT and JOINT++ that not only outperform baselines on the overall naturalness assessment

but also provide more subjectively consistent results for technical and rationality perspectives.

Our **contributions** can be summarized as follows:

- We take the first step to explore the naturalness of AI-generated images, focusing on five prevalent generative tasks. Our methods and findings can be applied to other forms of AI-generated multimedia.
- We contribute AGIN database, the first database that facilitates studying the naturalness of AI-generated images via human ratings on overall naturalness scores as well as the technical and rationality perspectives.
- Based on AGIN, we elucidate the mechanisms underlying human perception of image naturalness, providing insights into how technical and rationality factors influence human reasoning.
- We propose the JOINT, an objective naturalness evaluator for AI-generated images that models human perception on naturalness by a brain-inspired joint learning from technical and rationality perspectives, resulting in better performance.

2. Related Work

AI-generated Image and Naturalness. Generative models have emerged as an effective paradigm for image synthesis [62, 66, 73, 74, 76, 101]. Nonetheless, most generative adversarial network (GAN)-based methods [70, 99, 104] are prone to produce visually unnatural results due to their instability and mode collapse issues. Even state-of-the-art diffusion-based generative models [6, 41, 60, 92] introduce oftentimes perceptible unnatural perturbations such as spurious details, disordered layout, and color mismatch on images. Prior naturalness prediction approaches [24, 25, 55, 93, 111], driven by image statistic distribution, have predominantly focused on natural scene images (NSIs), which fail in AGIs, where exist diverse contextual content variations with less significant intrinsic properties (*e.g.* resolution, color space, and image format). As a result, it is challenging to design an effective image naturalness assessment method for AI-generated images that can be used to optimize the naturalness of the generated images and make them more robust to real-world applications.

AI-generated Image Assessment. Existing AI-generated image assessment research mainly focuses on the perceptual quality. Early objective metric such as Inception Score (IS) [77] measures perceptual quality by calculating the uniformity of AGIs group features from the output of Inception model. Distance-based methods such as Fréchet Inception Distance (FID) [31] and Kernel Inception Distance (KID) [4] as well as Precision-Recall [42] evaluate the discrepancy between distributions of AGI and NSI. Neverthe-

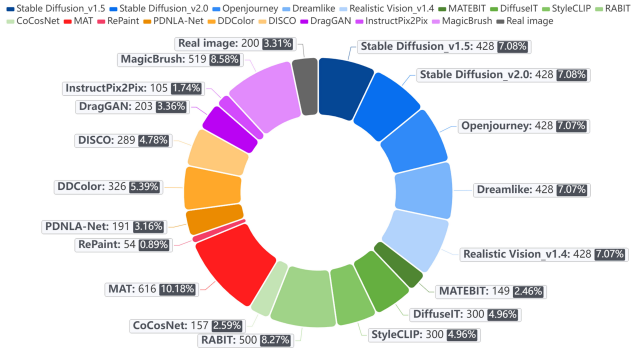


Figure 2. **Pie chart of AGIN database content distribution.** The blue, green, red, orange, purple, and black partitions indicate that the images are derived from text-to-image, image translation, image inpainting, image colorization, image editing, and real-world, respectively.

less, the above methods are all *group-targeted* and not suitable for assessing single image. Besides, the widely used CLIPScore [30] is already saturated in comparing state-of-the-art generative models with authentic images and can inflate for a model trained to optimize text-to-image alignment in the CLIP space [68]. This empirical evidence of the failure of the automatic measures motivates human evaluation of perceived quality. Kirstain *et al.* [40] collect human preferences between two generated images from the same prompt for text-to-image tasks. Wang *et al.* [85] investigate the impact of quality, fidelity, and correspondence of AI-generated images on human visual perception. Similarly, Li *et al.* [47] conduct a subjective evaluation to annotate images from both perception and alignment dimensions with varying input prompts and internal parameters in AGI models. However, these studies, which merely collect coarse, single-voice, and overall subjective opinions, lack the exploration of specific factors with fine-grained and explainable evaluations on various generation tasks.

3. AI-Generated Image Naturalness Database

In this section, we elaborate on the construction procedures of the proposed AGIN database, along with the subjective human evaluation (Fig. 3). The database includes 6,049 AI-generated images, on which we collected 907,350 ratings in terms of the overall naturalness score and its two perspectives: the technical and rationality score, as well as their respective main influencing factor.

3.1. Data Preparation

As an initial investigation, we choose five sources of AI-generated images including text-to-image, image translation, image inpainting, image colorization, and image editing, that typically suffer from naturalness problems. We select 18 models including: (1) *text-to-image*, 5 models with over 400 prompts are used for image generation. (2) *image*

translation, 5 models with various text-, image-, or mask-guided (e.g. edge map, semantic map) translation. (3) *image inpainting*, 2 models that take mutilated images as inputs. (4) *image colorization*, 3 models that colorize the grayscale images. (5) *image editing*, 3 models that perform layout or content editing on the image via text prompts or interactive anchor points. In addition to the AI-generated images, we also added 200 extra real images into the AGIN database to help analyze the accuracy of the subjective experiment and objective algorithms, which stand for a high level of naturalness. The distribution of the selected models and categories is displayed in the pie chart of Fig. 2. We carefully reproduce the generation processes in supplementary materials.

3.2. Design of the Human Evaluation

3.2.1 Choice of Naturalness-related Factors

We conduct the evaluation from two perspectives, *i.e.*, the low-level technical perspective and the high-level rationality perspective, as follows.

Factors in Technical Perspective. We consider specific image attributes (e.g. luminance and contrast) that have high correlations of naturalness [8, 24, 93]. Besides, *in-capture* authentic distortions [3, 97], such as reproduction of details and blur that happen in nature scene images, are considered. Concretely, we study four distortions:

(T-1) *Luminance*: Unrecognizable regions of images due to extremely high/low brightness [89].

(T-2) *Contrast*: High contrast produces a clearer and more vivid image, whereas low contrast leads to less color variety.

(T-3) *Detail*: Whether the image has detail or texture, such as wrinkles in clothing, hair, or skin.

(T-4) *Blur*: Clearness of image. Whether it is blurry or clear. and a common error introduced by the instability and mode collapse issues of generative models:

(T-5) *Artifacts*: Content discontinuity or meaningless objects [47, 59, 109, 114].

Factors in Rationality Perspective. Compared to real images, AGIs possess richer content with diverse styles. Beyond technical distortions, the visual naturalness of AGIs is largely affected by rationality-related factors [11, 59, 114]. Such high-level factors are vaguely described as *the memory of the real-life scene* in previous research [14, 17, 18, 44], which are not suitable for qualitative and quantitative analysis. In this work, we contribute 5 rationality dimensions to facilitate subjects to better rate their feeling on images.

(R-1) *Existence*: Whether the scene or objects in the image exist or could exist in the real world.

(R-2) *Color*: Does the image follow the natural color rule and present harmonious and pleasing colors?

(R-3) *Layout*: Is the image layout logical?

(R-4) *Context*: Whether the objects in the image are related.

(R-5) *Sensory Clarity*: The abstract perception. Whether the image content is easy to understand.

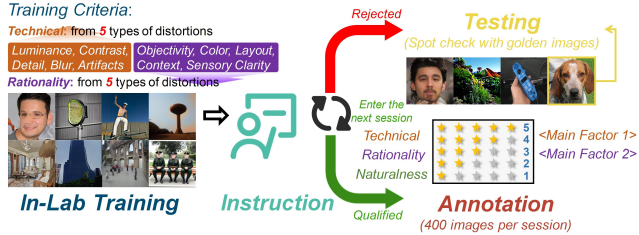


Figure 3. **Workflow of the in-lab human evaluation in AGIN.** It mainly includes four stages: 1) In-Lab Training, 2) Instruction, 3) Annotation, and 4) Testing, discussed in Sec. 3.2.2.

3.2.2 Design of the Study

Participants and Apparatus. To ensure the comprehensiveness and reliability of the evaluation, we recruited 30 participants (18 male, 12 female, age=22.6±3.1) from campus, all with normal (corrected) eyesight. We conduct the subjective studies in-lab to ensure that all subjects have a clear and consistent understanding of all factors. Each participant is compensated \$240 for evaluating 6,049 images. All images are displayed on a 27-inch screen with a resolution of 2560×1440 and a viewing distance of about 70cm.

Rating Strategy and Wording. We discuss the concrete form for human evaluation as follows. 1) *Task-oriented absolute choice.* Since the wording of questions and labels can significantly affect annotators’ labeling behavior, we abandon the traditional 3-point or 5-point Likert scale that only provides endpoint labels from *worst* to *best* and is too vague to describe the degree of naturalness. As a solution, we elaborate the questions and labels for three different perspectives to reduce subjectivity rather than using general ones (e.g. *bad*, *good*, or *very good*). 2) *Pick up the main factor.* Many existing subjective studies merely focus on the assessment of the overall score but neglect to explore the underlying factors. Therefore, we ask subjects to choose a primary factor that affects most for each perspective after rating the general scores, which enables us to investigate the correlation between each dimension and image naturalness.

Training, Testing, and Annotation. The workflow of the human evaluation is illustrated in Fig. 3. Before conducting the formal study, we manually generated 10 exemplars beyond the AGIN database for each dimension as training images to familiarize subjects with the goal of this evaluation. Subsequently, we instruct the subjects to rate the technical quality, rationality, and overall naturalness of each image from {1, 2, 3, 4, 5}, and select the main factors that most affect the technical quality and rationality perspectives. For testing, we randomly insert 10 *golden images* into each session as an inspection to ensure the quality of annotation. We defer more details of human evaluation and quality control of ratings to supplementary materials.

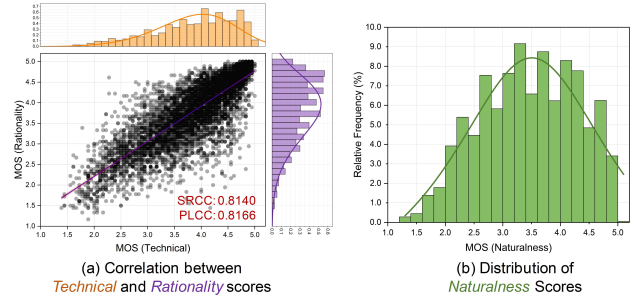


Figure 4. **Data properties of AGIN.** (a) The correlations between technical and rationality perspectives, and (b) distributions of overall naturalness scores.

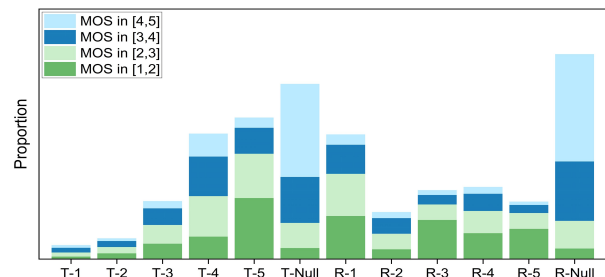


Figure 5. **Proportions for each dimension.** The tendency of main factors chosen by participants across different ranges of naturalness scores.

3.3. Insights

What affects the naturalness of AGIs? What are the latent correlations among different factors? Based on AGIN, we provide the following two insights:

Insight ①: *Naturalness is affected by both low-level technical distortions and high-level rationality distortions.*

We first provide a visualization of the data properties in AGIN database (Fig. 4a), from which we can observe the correlation between the technical perspective and the rationality perspective. Tab. 1 lists the quantitative results of Spearman and Pearson correlation between different perspectives, where the mean technical score, mean rationality score, and mean naturalness score are denoted as MOS_T , MOS_R , and MOS , respectively. It can be observed that the two perspectives affect naturalness unequally (i.e., rationality has a greater impact on the overall naturalness than technical perspective, while the linear weighted sum of two perspectives can better approximate the overall naturalness than any single form). This could lead to biased naturalness evaluation unwittingly when using mainstream IQA models that follow the overall MOS regression strategy.

Insight ②: *Factors in two perspectives are related, but have disparate impacts on naturalness scores.*

Fig. 5 shows the proportion of each factor in different ranges of naturalness scores, where *T-Null* and *R-Null* indicate that there exist no factors affecting naturalness or the subjects have difficulty in choosing the main factors. First, *T-Null* and *R-Null* are more prevalent in images with prefer-



Figure 6. Visualization of images with severe (1st row with red box) and minor effects (2nd row with green box) of each dimension.

Metrics	MOS _T	MOS _R	MOS _T + MOS _R	aMOS _T + bMOS _R
SRCC \uparrow	0.8647	0.9694	0.9672	0.9777
PLCC \uparrow	0.8599	0.9639	0.9580	0.9713

Table 1. **Correlation of perspectives.** The SRCC and PLCC between different perspectives and overall naturalness (MOS) for all 6,049 images in **AGIN**. a and b are 0.145 and 0.769, respectively.

able naturalness ($MOS \in [4, 5]$), indicating the impact of technical and rationality perspectives on naturalness. Additionally, we notice that humans are more sensitive to generated artifacts (T -5) and blur (T -4) in terms of technical quality while focusing more on the existence (R -1) of the image contents in terms of rationality. Furthermore, we find especial high proportions of artifacts (T -5), existence (R -1), and layout (R -3) in the case of poor naturalness ($MOS \in [1, 2]$), suggesting that they are important naturalness factors for AGIs to take into account. Considering the inter-relation between technical quality and rationality, we speculate that severe artifact distortions may lead to irrational content and chaotic layout. We also provide examples with varying degrees of effect for each dimension in Fig. 6, to better illustrate the manifestations of the naturalness problem in different dimensions. Overall, these newly contributed dimensions describe naturalness concerns of AGIs, some of which have never been encountered in conventional IQA domain, providing reliable intuitions for developing objective naturalness assessment models.

4. The Proposed JOINT and JOINT++

Studies in neurosciences [22, 33, 67] suggest that humans possess two distinct visual systems, which follow two main pathways, *i.e.*, the dorsal stream and ventral stream, to handle low-level and high-level visual perception, respectively. *To align model behavior with human perception process*, we propose the **Joint Objective Image Naturalness evaluator (JOINT)** that models human naturalness reasoning by simultaneously considering the impact of technical and rationality perspectives, shown in Fig. 7.

Specifically, the technical perspective mainly refers to the low-level distortions, *e.g.*, *texture losses*, *blurs*, and *artifacts* [1, 81, 88, 89], while the rationality of image is largely related to high-level visual information including *semantic*,

attribute theme, and *layout* that are also the key elements of aesthetic assessment [28, 29, 49, 95]. Notably, some of the perceptual factors are related to both perspectives, such as *contrast* that belongs to technical distortion and can affect *color* harmonization, or *artifacts* (a generative technical distortion but highly coupled with the *existence* and *layout* of the image contents). *To allocate two branches with corresponding learning interests*, we present several specific designs (*e.g.*, *patch partition*, *feature regularization*) and two different training schemes, illustrated as follows.

4.1. The Technical Prior Branch

For technical prior branch, we explicitly guide the model to prioritize the technical distortions while minimizing the impact of semantic information. Concretely, we randomly crop the image \mathcal{I} into size-fixed patches and stitch them together (\mathcal{I}_{rand}) to disorganize most contents and layout while retaining technical distortions, thus destroying semantic information and rationality factors in images [87, 88]. However, different from most global technical distortion, generated *artifacts* could become unrecognizable by random patch partition. Therefore, we *localize possible perceptual artifacts* first and bypass these regions to keep their local distortion information.

Perceptual Artifacts-guided Patch Partition. Numerous research efforts have sought to localize the edited regions [86, 110], which basically involves training a model to pinpoint systematic inconsistencies in generated images. More recently, Zhang *et al.* [102, 109] further expand this task to a fine-grained level that not only predicts inpainted areas but also detects and segments artifact areas that are noticeable to human perception. In this work, we use the detection model provided in [109] as the artifacts extractor to guide the patch partition. *Note that we do not focus on the detection process in this work.* Specifically, given an image \mathcal{I} of size $\mathcal{I}_W \times \mathcal{I}_H$, the patch partition can be formulated as:

$$m, n = AExtractor(\mathcal{I}), \quad (1)$$

$$\mathcal{I}_{rand} = RPart\left(\mathcal{I}_{j \in [1, \frac{\mathcal{I}_H}{N_8}] \setminus \{m\}, k \in [1, \frac{\mathcal{I}_W}{N_8}] \setminus \{n\}}, N_8\right), \quad (2)$$

where $AExtractor(\cdot)$ denotes the perceptual artifacts location extractor that returns coordinates for artifacts in m -th

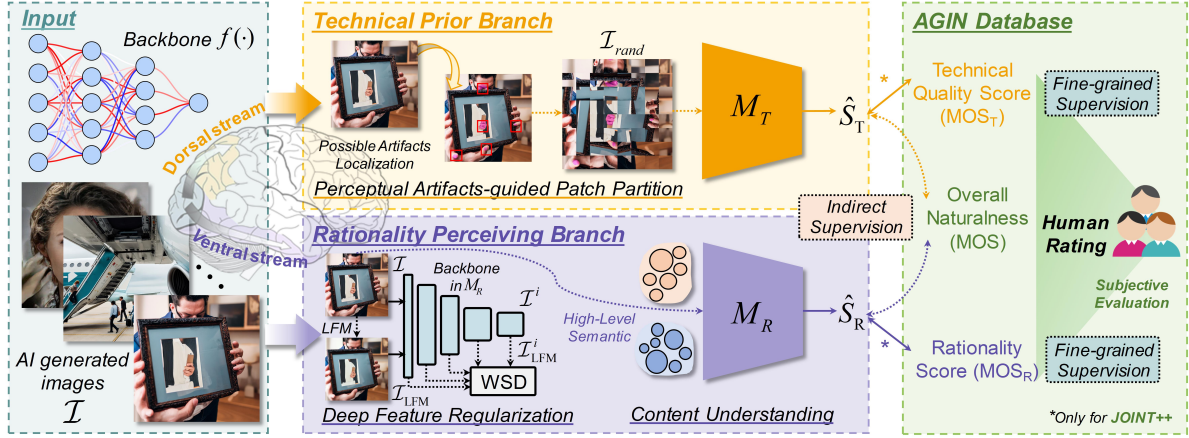


Figure 7. **Framework of the proposed JOINT and JOINT++ with joint learning strategy.** It consists of the technical prior branch (Sec. 4.1) and the rationality perceiving branch (Sec. 4.2). More details can be found in supplementary materials.

horizontal grid and n -th vertical grid. The divided patch size is $N \times N$. $RPart(\cdot, N_8)$ denotes a random partition within the 8-connected neighborhood of the patch, which destructs the local semantic information of the image while preserving the global semantics.

4.2. The Rationality Perceiving Branch

Since the high-level semantic information of rationality concerns is likewise of interest to the image aesthetic assessment (IAA), we pre-train this branch first with IAA database and introduce a deep feature regularization to mitigate the effect of technical quality.

Deep Feature Regularization. To maintain the principal content of the image and filter out the impact of partial technical factors, we use the piece-wise smooth algorithm [2] to obtain the low-frequency map of images \mathcal{I}_{LFM} . Moreover, existing research [52, 105] suggest that the distribution differences of deep features among different stages are related to technical distortions. Henceforth, we employ the one-dimension form of Wasserstein Distance (WSD) [10] as a penalty constraint \mathcal{L}_{WSD} to eliminate the technical interference in rationality measuring by reducing the feature distribution divergence between \mathcal{I} and \mathcal{I}_{LFM} :

$$\mathcal{L}_{WSD} = W_l(\mathcal{I}, \mathcal{I}_{LFM}) + \sum_{i=1}^N W_l(\mathcal{I}^i, \mathcal{I}_{LFM}^i), \quad (3)$$

where \mathcal{I}^i and \mathcal{I}_{LFM}^i denote the extracted features of \mathcal{I} and \mathcal{I}_{LFM} at the i -th stage. $W_l(\cdot, \cdot)$ is the Wasserstein distance with l -norm.

4.3. Learning Objectives

We have discussed in Sec. 3.3 that the overall naturalness score MOS can be approximated as a weighted sum of MOS_T and MOS_R . Here, we propose an indirect supervision (\mathcal{L}_{IS}) scheme to optimize two branches using the over-

all naturalness MOS. However, the subjective bias in two perspectives can cause large absolute prediction errors and reduce the prediction accuracy for each branch. Inspired by [46, 48, 88], we add the Spearman Rank-order Correlation Coefficient (SRCC) loss as a restraint to boost the prediction monotonicity of models. Overall, JOINT learns to assess image naturalness by jointly optimizing:

$$\mathcal{L}_C = \mathcal{L}_{MSE} + \alpha \mathcal{L}_{SRCC}, \quad (4)$$

$$\mathcal{L}_{IS} = \mathcal{L}_C(\hat{S}_T, MOS) + \mathcal{L}_C(\hat{S}_R, MOS) + \beta \mathcal{L}_{WSD}, \quad (5)$$

where α and β are hyperparameters to control the strength of \mathcal{L}_{SRCC} and \mathcal{L}_{WSD} , respectively. \hat{S}_T and \hat{S}_R denote the predicted score of technical and rationality branch. Besides, based on the AGIN database, we also propose a fine-grained version (\mathcal{L}_{FS}) using the corresponding perspective opinions for both branches:

$$\mathcal{L}_{FS} = \mathcal{L}_C(\hat{S}_T, MOS_T) + \mathcal{L}_C(\hat{S}_R, MOS_R), \quad (6)$$

and the proposed JOINT++ is trained by a combination of the above two losses so as to obtain more accurate predictions for both branches:

$$\mathcal{L}_{JOINT++} = \mathcal{L}_{FS} + \lambda_{IS} \mathcal{L}_{IS} \quad (7)$$

Subjective Weighting Strategy. According to the subjective study in AGIN, we adopt a simple but effective weighting strategy to compute the overall naturalness prediction (\hat{S}_N) from two perspectives: $\hat{S}_N = 0.145\hat{S}_T + 0.769\hat{S}_R$. With better performance in experiments, this strategy further demonstrates the observations in Sec. 3.3.

5. Experiments

In this section, we conduct experiments to verify: (1) the necessity of AGIN database (Sec. 5.2). (2) can JOINT and JOINT++ better assess the overall naturalness of AGIs (Sec. 5.3)? Moreover, ablation studies are included (Sec. 5.4).

Methods	Type	Pre-computed Statistics/ Pre-training Datasets	Technical		Rationality		Naturalness	
			SRCC \uparrow	PLCC \uparrow	SRCC \uparrow	PLCC \uparrow	SRCC \uparrow	PLCC \uparrow
BRISQUE (TIP, 2012) [63]	Traditional IQA (handcraft features)	KonIQ-10k [32]	0.3544	0.3602	0.1268	0.1299	0.1618	0.1660
NIQE (SPL, 2013) [64]		KonIQ-10k [32]	0.1843	0.1484	0.0377	0.0235	0.0707	0.0445
*DBCNN (TCSVT, 2018) [106]		TID2013 [71]	0.2664	0.3138	0.0888	0.1199	0.1209	0.1376
-- same as above --		LIVE Challenge [21]	0.4132	0.4903	0.1518	0.2082	0.1993	0.2422
HyperIQA (CVPR, 2020) [80]	Deep IQA (deep features)	KonIQ-10k [32]	0.4951	0.5252	0.2275	0.2492	0.2786	0.2956
* MUSIQ (ICCV, 2021) [38]		KonIQ-10k [32]	0.4953	0.5541	0.2839	0.3211	0.3332	0.3725
-- same as above --		PaQ-2-PiQ [96]	0.4329	0.4709	0.2061	0.2399	0.2443	0.2799
		KonIQ-10k [32]	0.4817	0.5262	0.2512	0.2847	0.2951	0.3271
		SPAQ [20]	0.4324	0.5166	0.2193	0.2741	0.2561	0.3085
		ImageNet [75]	0.5178	0.5756	0.2912	0.3324	0.3339	0.3735
UNIQUE (TIP, 2021) [107]	Deep IAA (deep features)	KADID-10k [53]	0.4154	0.4214	0.2733	0.2655	0.3003	0.3001
*MANIQA (CVPRW, 2022) [94]		KonIQ-10k [32]	0.5771	0.5902	0.3453	0.3594	0.3937	0.4034
-- same as above --		PIPAL2022 [23]	0.4014	0.4407	0.1985	0.2354	0.2341	0.2597
		PsychoFlickr [16]	0.1363	0.1234	0.2445	0.2587	0.2261	0.2298
PAIAA (TIP, 2020) [49]		TAD66k [29]	0.1894	0.2015	0.2774	0.2803	0.2530	0.2619
TANet (IJCAI, 2022) [29]	Deep IAA (deep features)	AVA [65]	0.2549	0.3142	0.2348	0.2278	0.2232	0.2583
Delegate Transformer (ICCV, 2023) [28]		BAID [95]	0.0515	0.0359	0.1477	0.1380	0.1413	0.1456
SAAN (CVPR, 2023) [95]		WTF-400M	0.2114	0.3275	0.0348	0.0827	0.0167	0.1109
CLIP-IQA (AAAI, 2023) [84]	CLIP-based model (visual language prior)	WIT-400M+KonIQ-10k [32]	0.4959	0.5595	0.2613	0.3189	0.3078	0.3550
CLIP-IQA ⁺ (AAAI, 2023) [84]		hybrid [15, 21, 32, 43, 53, 78]	0.4928	0.5428	0.2457	0.2765	0.2974	0.3244
LIQE (CVPR, 2023) [108]		Q-Instruct [90]	0.4741	0.5085	0.3074	0.3271	0.3268	0.3566
InternLM-XComposer (arxiv, 2023) [103]		AGIN _{train}	0.8173	0.8235	0.7564	0.7711	0.7986	0.8028
JOINT (Ours)	Deep INA (deep features)	AGIN _{train}	0.8351	0.8429	0.8033	0.8127	0.8264	0.8362
JOINT++ (Ours)								

Table 2. **Validating the necessity of AGIN database.** All baselines are trained using datasets from their respective domains. **Red, Blue,** and **Black** indicate the best, second, and third best performance, respectively.

5.1. Experimental Settings

Databases and Baselines. We conduct experiments on our proposed AGIN database and select 15 state-of-the-art methods as references to be compared against, including two traditional NR-IQA methods: BRISQUE [63] and NIQE [64]; five deep NR-IQA methods: DBCNN [106], HyperIQA [80], MUSIQ [38], UNIQUE [107], and MANIQA [94]; four deep image aesthetic assessment (IAA) methods: PAIAA [49], TANet [29], Delegate Transformer [28], and SAAN [95]; four contrastive language-image pre-training (CLIP) model-based IQA methods: CLIP-IQA [84], CLIP-IQA⁺ [84], LIQE [108], and InternLM-XComposer [103].

Implementation Details. In the technical branch, we crop patch at size 64×64 , and Swin Transformer [56] is used as backbone. We use the ResNet50 backbone [27] pre-trained with AVA [65] in the rationality branch. α is set as 1. β and λ_{IS} are set as 0.5. We train our model for 30 epochs using the Adam optimizer [39] with learning rate 2×10^{-5} . The batch size is set to 32. All experiments are conducted under 5 train-test splits.

5.2. Exploring the Necessity of AGIN Database

In this section, we conduct experiments to verify whether the existing IQA and IAA databases can solve the problem of AI-generated image naturalness assessment, *i.e.*, the necessity of AGIN database. Specifically, we test the baselines on AGIN using their respective pre-trained models. We can obtain the following observations from Tab. 2: (1) Our AGIN database is of great importance for assessing the naturalness of AI-generated images. The proposed JOINT++ outperforms MANIQA [94], the second-

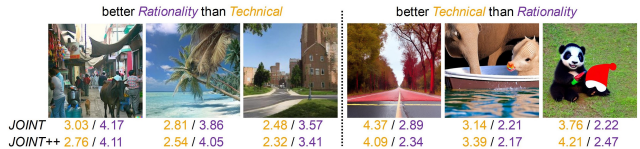


Figure 8. **Qualitative Studies of JOINT and JOINT++.** Visualizations of images in the AGIN that have opposite technical quality and rationality. Zoom-in for better visualization.

best method pre-trained on KonIQ-10k [32], by 0.4327 (+109.91%) in SRCC and 0.4328 (+107.29%) in PLCC, which shows the inferiority of existing IQA, IAA, visual-language models as well as datasets in evaluating the naturalness of AI-generated images. (2) Evaluating images from technical and rationality perspectives exhibits significant differences. We notice that IQA methods show relatively better performance in evaluating technical quality, whereas IAA methods excel in assessing rationality, which underscores the necessity of our distinct exploration of each perspective in the AGIN database. (3) Image naturalness assessment is different from both quality assessment and aesthetic assessment. Since mainstream IQA and IAA approaches fail to provide subjectively consistent evaluation results for image naturalness (more than 105% lower in SRCC/PLCC), we speculate that this is due to the diverse characteristics of the image sources and disparities in task objectives, illustrating the necessity of constructing AGIN and exploring the influencing factors.

5.3. Evaluation on the AGIN

Quantitative Studies. We benchmark recent state-of-the-art IQA and IAA methods by conducting training and testing in the AGIN. As shown in Tab. 3, the two classical IQA

Methods	Technical		Rationality		Naturalness	
	SRCC \uparrow	PLCC \uparrow	SRCC \uparrow	PLCC \uparrow	SRCC \uparrow	PLCC \uparrow
BRISQUE [63]	0.4867	0.4909	0.3608	0.3684	0.3745	0.4067
NIQE [64]	0.4235	0.4279	0.3144	0.3211	0.3358	0.3378
DBCNN [106]	0.7623	0.7661	0.6834	0.6838	0.7057	0.7128
HyperIQA [80]	0.7752	0.7806	0.7196	0.7292	0.7365	0.7509
MUSIQ [38]	0.7286	0.7355	0.6974	0.7013	0.7066	0.7103
UNIQUE [107]	0.7358	0.7434	0.6583	0.6685	0.6772	0.6789
MANIQA [94]	0.7763	0.7817	0.7192	0.7217	0.7385	0.7343
PAIAA [49]	0.4763	0.4833	0.4532	0.4596	0.4483	0.4528
TANet [29]	0.5367	0.5587	0.4731	0.4762	0.4782	0.4535
Del. Transf. [28]	0.5882	0.6134	0.5037	0.4942	0.4805	0.4961
SAAN [95]	0.4299	0.4380	0.4009	0.4160	0.4196	0.4184
JOINT (Ours)	0.8173	0.8235	0.7564	0.7711	0.7986	0.8028
JOINT++ (Ours)	0.8351	0.8429	0.8033	0.8127	0.8264	0.8362

Table 3. **Performance comparisons on the AGIN.** We retrained all models using the score of each corresponding perspective.

Perspective/ Variants/Metric	Technical		Rationality		Naturalness	
	SRCC \uparrow	PLCC \uparrow	SRCC \uparrow	PLCC \uparrow	SRCC \uparrow	PLCC \uparrow
<i>w/o</i> Localization	0.811	0.816	0.755	0.769	0.782	0.794
<i>w/o</i> Regularization	0.814	0.820	0.729	0.738	0.758	0.766
<i>w/o</i> Multi-perspective	0.768	0.781	0.703	0.712	0.727	0.733
JOINT (Ours)	0.817	0.824	0.756	0.771	0.799	0.803

Table 4. **Ablation study of JOINT (I):** the effects of specific designs in technical and rationality branches.

Variants	Technical		Rationality		Naturalness	
	SRCC \uparrow	PLCC \uparrow	SRCC \uparrow	PLCC \uparrow	SRCC \uparrow	PLCC \uparrow
\hat{S}_T \hat{S}_R \oplus	0.817	0.824	0.720	0.724	0.725	0.744
\checkmark	0.687	0.699	0.756	0.771	0.767	0.763
\checkmark \checkmark	0.753	0.768	0.732	0.744	0.759	0.755
\checkmark \checkmark \checkmark	0.711	0.723	0.746	0.762	0.799	0.803

Table 5. **Ablation study of JOINT (II):** correlation between perspectives and the effect of subjective weighting (denoted as \oplus).

methods [63,64] perform significantly worse than deep IQA methods, and the proposed JOINT++ still achieves the best performance in terms of technical, rationality, and overall naturalness assessment. Surprisingly, all IAA methods exhibit subpar performance that on average 44.74%/45.56% lower than JOINT++ in naturalness evaluation. Their ineffectiveness can be attributed to a lack of consideration for technical factors and an attention bias in understanding the semantics of the content itself. Besides, most IAA models aim to learn more about global information (*e.g.*, *semantic, composition*) than local elements that could overwhelmingly affect naturalness. Furthermore, both IQA and IAA approaches solely consider a single perspective with highly coupled factors in image naturalness reasoning, thereby rendering them incapable of providing reliable results.

Qualitative Studies. As shown in Fig. 8, we visualize two typical scenarios where the predicted technical and rationality scores are significantly diverged. The images on the left with better rationality scores depict more realistic scenes yet suffer from *noise, blur, artifacts*. In contrast, the images on the right with better technical scores are rich in details but with *irrational colors, nonexistent contents, and irrelevant objects*. These observations align with human perception of the two perspectives, further substantiating the effectiveness and necessity of our joint learning strategy that can provide subjectively consistent image naturalness predictions.

Loss Function	Technical		Rationality		Naturalness			
	\mathcal{L}_{IS}	\mathcal{L}_{FS}	SRCC \uparrow	PLCC \uparrow	SRCC \uparrow	PLCC \uparrow		
\checkmark			0.817	0.824	0.756	0.771	0.799	0.803
	\checkmark		0.831	0.834	0.786	0.794	0.819	0.828
\checkmark	\checkmark		0.835	0.843	0.803	0.813	0.826	0.836

Table 6. **Ablation study of JOINT++:** the learning objectives.

5.4. Ablation Studies

Effects of Specific Designs. In Tab. 4, we verify the effect of three special designs in JOINT by keeping other parts the same. First, it is superior to the variant *w/o Localization* that randomly shuffles the patches and destruct the perceptual artifact regions, showing the necessity of preserving the local artifact distortion information. Secondly, with the deep feature regularization, JOINT is able to focus more on the rationality perspective. Furthermore, JOINT is notably better than the variant *w/o Multi-perspective* that directly takes the original images as inputs of both branches, proving the effectiveness of multi-perspective joint learning strategy.

Effects of Subjective Weighting Strategy. We discuss the subjective weighting strategy in Tab. 5. It can be observed that any single branch can not adequately represent the naturalness, and directly taking $\hat{S}_T + \hat{S}_R$ as overall naturalness without weighting will also bring a notable performance decrease ($-5.01\%/ -5.98\%$ in terms of SRCC/PLCC), which further supports the observations found in the AGIN.

Effects of Learning Objectives. As shown in Tab. 6, supervised by corresponding MOS labels yields more accurate predictions. Compared with \mathcal{L}_{IS} , \mathcal{L}_{FS} achieves around $+1.71\%/+1.21\%$, $+3.97\%/+2.98\%$, and $+2.50\%/+3.11\%$ performance gains in terms of technical, rationality, and naturalness assessment, respectively. It is also worth noting that combining \mathcal{L}_{IS} with \mathcal{L}_{FS} can significantly improve the prediction accuracy of overall naturalness. Additionally, even without MOS labels for each perspective, \mathcal{L}_{IS} can still achieve comparable performance, which suggests the feasibility of modeling the mechanisms of human perception of naturalness using both perspectives.

6. Conclusion

In this paper, we contribute AGIN database and the first subjective evaluation aimed at exploring the impact of technical and rationality perspectives on the naturalness of AGIs. Besides, we propose JOINT and JOINT++, the objective naturalness evaluators that achieve higher alignment with human opinions against existing IQA and IAA approaches. Our work benefits community by 1) presenting AGIN, which enables research on benchmarking and evaluating naturalness of AGIs by multi-dimensional human ratings; 2) encouraging new research on the naturalness assessment of AGIs via analysis of technical and rationality features; 3) promoting the development of better INA algorithms for AGIs or other forms of AI-generated multimedia.

Database	Image Source	#Content	#Image	Perspective	Distortion
LIVE (2004) [78]	Kodak test set	30	779	Quality	5 Artificial
TID2008 (2008) [72]	Kodak test set	25	1,700	Quality	17 Artificial
CSIQ (2009) [43]	Kodak test set	30	866	Quality	6 Authentic
TID2013 (2013) [71]	Kodak test set	25	3,000	Quality	24 Artificial
LIVEC (2015) [21]	Camera	1162	1162	Quality	15 Authentic
WED (2017) [61]	Internet	4,744	94,880	Quality	4 Artificial
MDID (2017) [82]	Internet	20	1,600	Quality	5 Artificial
KADID-10k (2019) [53]	Internet	81	10,125	Quality	25 Artificial
KonIQ-10k (2020) [32]	Multimedia	10,073	10,073	Quality	– Authentic
PAN (2023) [50]	Autonomous Driving	2,688	2,688	Naturalness	– Adversarial
AGIN (Ours)	AI-generated	6,049	6,049	Technical+Rationality+Naturalness	18 Generative

Table 7. Comparisons between the **AGIN** database and existing IQA databases.

Baseline	Model	Generator	Resolution	#Content	Input Source
Text-to-Image	Stable Diffusion_v1.5 (CVPR’22) [74]	Diffusion	512 ²	428	Prompts are from COCO Caption [54] , DrawBench [76] , and ChatGPT.
	Stable Diffusion_v2.1 (CVPR’22) [74]	Diffusion	512 ²	428	
	Openjourney [62, 74]	Diffusion	512 ²	428	
	Dreamlike [19, 74]	Diffusion	768 ²	428	
	Realistic Vision_v1.4 [74]	Diffusion	512 ²	428	
Image Translation	RABIT (ECCV’22) [99]	GAN	256 ² \triangleright 512 ²	500	ADE20K [113]
	DiffuseIT (ICLR’23) [41]	Diffusion	256 ² \triangleright 512 ²	300	Landscape [13]
	StyleCLIP (ICCV’21) [70]	GAN	1024 ²	300	FFHQ [36]
	MATEBIT (CVPR’23) [34]	GAN	512 ²	149	CelebA-HQ [58]
	CoCosNet (CVPR’20) [104]	GAN	512 ²	157	CelebA-HQ [58]
Image Inpainting	RePaint (CVPR’22) [60]	Diffusion	512 ²	54	CelebA-HQ [58]
	MAT (CVPR’22) [51]	GAN	512 ²	616	CelebA-HQ [58], Places [112]
Image Colorization	PDNLA-Net (TIP’23) [83]	GAN	512 ²	191	ADE20K [113]
	DDColor (ICCV’23) [35]	VAE	\geq 512 ²	326	Imagenet [75]
	DISCO (SIGGRAPH’22) [92]	Diffusion	512 ²	289	COCO [54]
Image Editing	DragGAN (SIGGRAPH’23) [69]	GAN	512 ²	203	DeepFashion [57]
	InstructPix2Pix (CVPR’23) [6]	Diffusion	\geq 512 ²	105	ADE20K [113], Landscape [13]
	MagicBrush (arXiv’23) [100]	GAN+Diffusion	1024 ²	519	COCO [54]

Table 8. **Detailed information of the models used in AGIN.** “ \triangleright ” indicates the upsampling operation.

Appendix

A. Extended Details of AGIN Database

In this section, we provide additional details for the construction of the AGIN database. We define the task of evaluating the naturalness of AI-generated images as a special case of image quality assessment (IQA). As shown in Tab. 7, AGIN differs from the existing IQA database in three aspects: image source, evaluation perspective, and distortion type. Previous IQA databases mainly focus on *post-capture* artificial distortion (e.g., masked noise, JPEG compression) or *in-capture* authentic distortions (e.g., motion blur, exposure), while AI-generated images possess entirely different generative patterns and richer contents, posing new challenges for constructing a comprehensive database. Since we focus on the naturalness assessment of AI-generated images, only prompts that describe objective objects or phenomena and source images with authentic style are used

to build the database. It is unnecessary to add abstract or surreal concepts, which are prone to appear unnatural. To cover diverse appearances of naturalness issues, we collect multi-sourced images from five tasks, as depicted in Tab. 8. Exemplar images for each model are shown in Fig. 9.

A.1. Collecting AI-generated Images

Detailed Information of Text-to-Image Models. For text-to-image models, we first choose 20 hot keywords from the *PNGIMG* website¹ and then create 10 prompts using GPT3.5 for each keyword with the following query:

I want you to act as a prompt generator for the text-to-image program. Your job is to provide detailed, accurate, and real descriptions that do exist in the real world and will inspire unique and true-life images from the AI. Now you can

¹<https://pngimg.com>

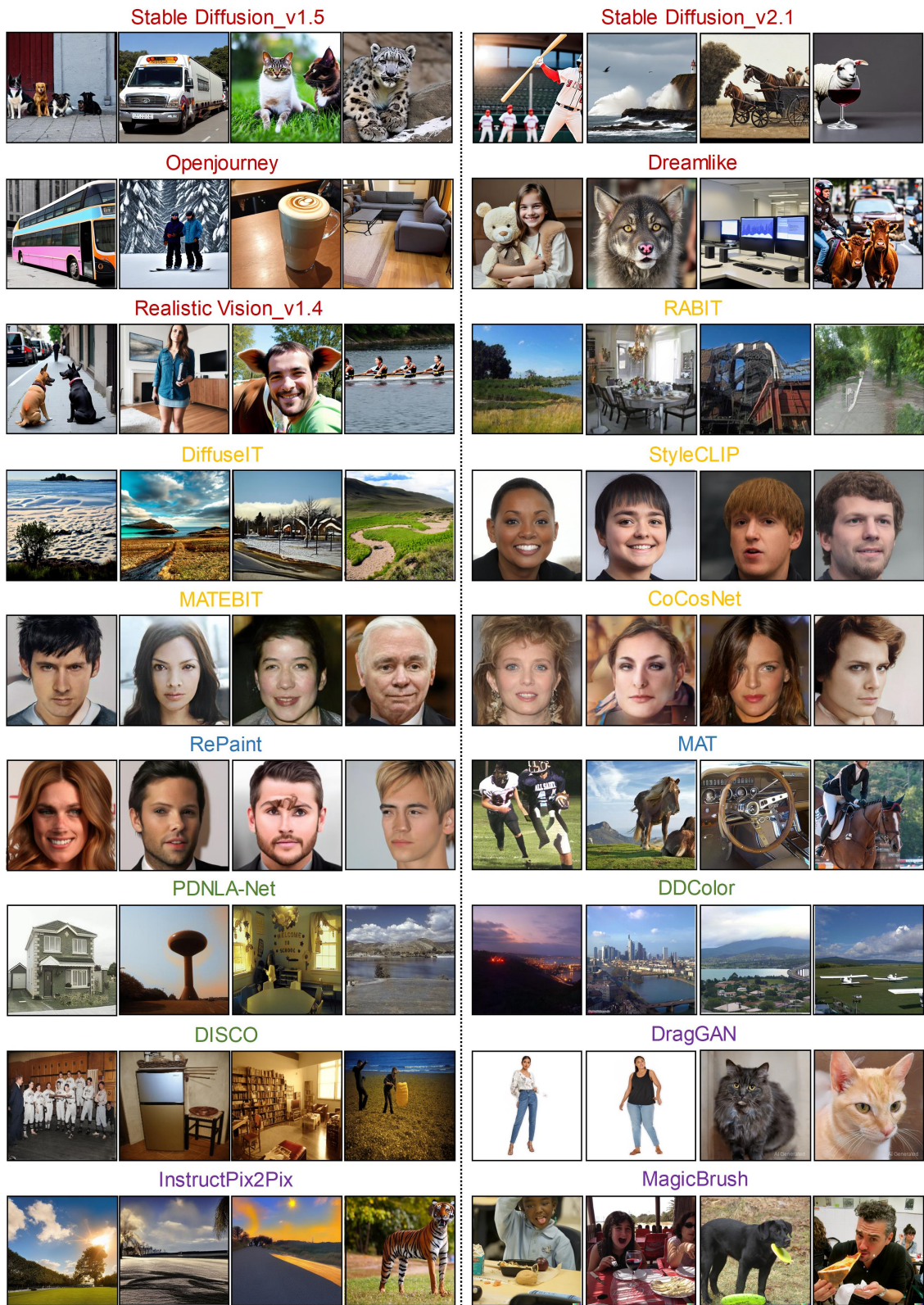


Figure 9. **Additional results on generated images in AGIN database.** We show four examples for each model in five tasks (text-to-image, image translation, image inpainting, image colorization, and image editing). Zoom-in for better viewing.

provide 10 detailed, accurate, and real descriptions (within 35 words) according to the keyword: <keyword>.

Keywords: nature, festival, food, animals, flower, people, space, travel, book, vehicles, artifacts, fruits, clothing, object, sport, electronics, transportation, architecture, drinks, human face.

At times, the generated prompts are too obscure or too similar, so we manually examine the text compliance and restart the prompt generation process iteratively. We also randomly sample 100 captions from the COCO [54] dataset and choose 128 proper prompts from the commonly used DrawBench [76] by excluding inappropriate categories (e.g. conflicting, misspellings, and rare words). Concretely, we select mainstream text-to-image models including Stable Diffusion v1.5² [74], Stable Diffusion v2.1³ [74], Openjourney⁴ [62, 74], Dreamlike⁵ [19, 74], and Realistic Vision v1.4⁶ [74], to generate photorealistic images of the aforementioned prompts. Note that in real-world scenarios, people aim to use AI to obtain high-quality images without visual defects. Thus, we intentionally avoid using specialized prompt suffixes such as *8K*, *HDR*, *photographic*, to simulate scenarios where naturalness issue occurs.

Detailed Information of Image Translation Models. We choose five up-to-date image translation models including RABIT [99], DiffuseIT [41], StyleCLIP [70], MATEBIT [34], and CoCosNet [104], to investigate the manifestation of naturalness issues in image translation tasks. For RABIT, MATEBIT, and CoCosNet, we take different conditional inputs (e.g., edge map, semantic map) and exemplars provided by ADE20K [113] and CelebA-HQ [58] datasets to generate translation results. For DiffuseIT, we use the pre-trained diffusion model provided by the authors and adopt both text-guided and image-guided strategies to achieve image translation, where target and source images are sampled from Landscape [13] dataset. Conditional prompt keywords such as *beach*, *snow*, *desert*, *sea*, *mountain*, *cloud*, and *grassfield*, are applied to improve the diversity of outputs. For StyleCLIP, we perform attribute changes including facial expression, hairstyle, skin color, and makeup, on the portraits of celebrities from FFHQ [36] dataset using the pre-trained StyleGAN2 [37].

Detailed Information of Image Inpainting Models. Image inpainting, also known as image completion, aims at filling missing regions reasonably within an image while

²<https://huggingface.co/runwayml/stable-diffusion-v1-5>

³<https://huggingface.co/stabilityai/stable-diffusion-2-1>

⁴<https://openjourney.art/>

⁵<https://huggingface.co/dreamlike-art/dreamlike-photoreal-2.0>

⁶https://huggingface.co/SG161222/Realistic_Vision_V1.4

maintaining harmonization with the rest of the image. Inpainting approaches thus require strong generative capabilities, otherwise, it can lead to poor results with severe naturalness distortion. Here, we randomly select input contents from CelebA-HQ [58] and Places [112] datasets and generate 54 and 616 images using RePaint [60] and MAT [51], respectively. Partial brushes, squares, or even masks with large missing areas are employed to enhance the diversity of generated contents. We notice that both two models struggle in processing complex scenes with multiple objects due to the lack of sufficient semantic understanding. Most of the generated images have various degrees of artifacts and unreasonable layouts, which highlights the necessity to evaluate the naturalness of images.

Detailed Information of Image Colorization Models.

Compared to the complete image generation task, image colorization aims to restore two missing color channels on the basis of grayscale images, which usually suffers from ambiguity and uncertainty. In other words, an object may accept multiple distinct colors while keeping the semantic consistency among pixels. Such characteristics predispose it to be a hard-hit area of naturalness problems. For this reason, we select three representative models including PDNLA-Net [83], DDColor [35], and DISCO [92], to reflect this phenomenon. Specifically, we extract source images from ADE20K [113], Imagenet [75], and COCO [54] datasets and manually convert them to grayscale as input.

Detailed Information of Image Editing Models. There exists a huge demand for providing flexible and controllable image editing means in daily life, ranging from individual users to professional applications. Improper instruction may cause unnaturalness between the edited areas and surrounding contents. Here, we choose the well-known text-guided image editing model (InstructPix2Pix [6]) and an interactive model (DragGAN [69]) to generate natural or unnatural images. For InstructPix2Pix, we apply text instructions, such as “*add sth to sth*”, “*turn it into sth*”, “*replace sth the with sth*”, to edit images. The source images are from ADE20K [113] and Landscape [13] datasets. For DragGAN, we choose images from the DeepFashion [57] dataset and set up two anchor points with certain drag directions. Then, DragGAN will move the handle point to reach its corresponding target point, thus completing the image editing procedure. Moreover, we extract 519 images from MagicBrush [100], a large-scale, manually annotated dataset for instruction-guided real image editing. Since it already covers diverse editing scenarios, we do not re-process these images.

A.2. Detailed Information of Human Evaluation

Laboratory Setup. Considering the viewing effect, a 27-inch Lenovo monitor with 2560×1440 resolution is used for image display. The viewing distance and optimal horizontal

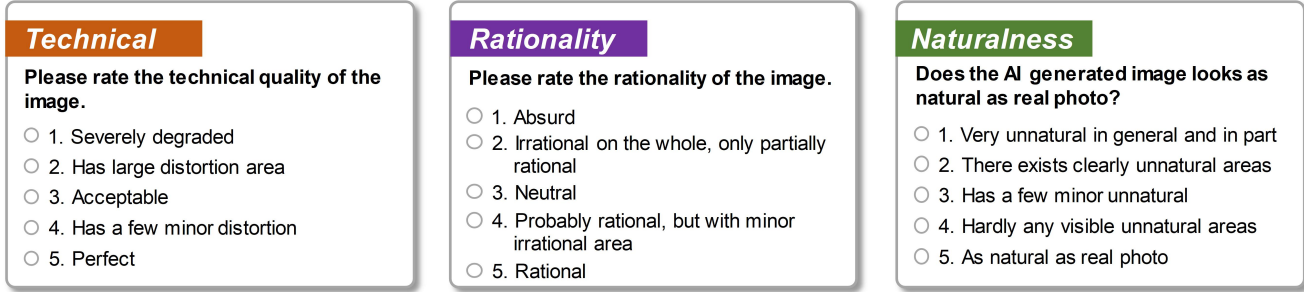


Figure 10. **Question and labels of three candidate task designs.** Instead of using typical labels for a 5-point Likert scale, we elaborate questions and labels for the rating of technical quality, rationality, and naturalness.

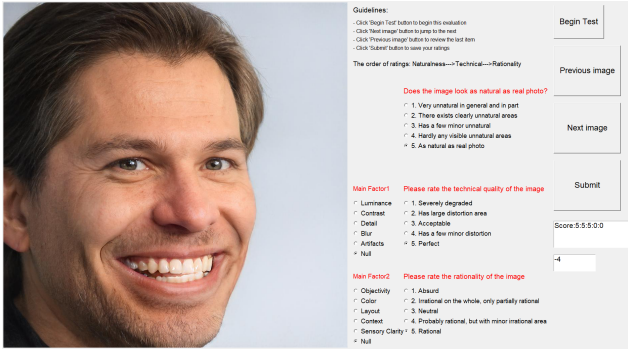


Figure 11. **The interface for human evaluation interface.** Subjects are required to rate the technical quality, rationality, and naturalness of AGIs, and select the corresponding main factor through the radio buttons.

viewing angle are set as 1.9 times the height of the display ($\approx 70\text{cm}$) and $[31^\circ, 58^\circ]$, respectively. Other settings such as ambient brightness, lighting, and background are configured according to the ITU-R BT.500 recommendation [7].

Interface Design and Stimuli Presentation. As shown in Fig. 11, the interface layout is mainly composed of the left image display area and the right operation area, which allows viewers to browse the previous/next image and select the most appropriate options. We adopt the single-stimulus procedure for naturalness assessment and require the participant to focus on and evaluate the overall naturalness, as well as the technical quality and rationality of the images. To avoid the interference of rating technical quality and rationality on naturalness collection, the evaluation of each image follows a 2-phase process. Firstly, an image is selected from AGIN database and participants are asked to evaluate the overall naturalness. Secondly, only after the naturalness evaluation is complete can participants move on to rate the technical quality and rationality of the image, as well as to select their respective main factors. Specifically, we design questions and labels for three different tasks as shown in Fig. 10, which affects participants’ labeling be-

havior and enables us to obtain more accurate data. Besides, to maximize the rating efficiency, participants were asked to click 1-5 radio buttons directly instead of using the keyboard to enter.

Formal Study. Each participant was required to evaluate 6,049 images from three perspectives and to select two main factors, yielding a total of $6,049 \times 30 \times (3 + 2) = 907,350$ ratings. Note that we shuffle and randomly divide all images into 15 sessions, each session except the 15th contains 400 images. During the study, all subjects go through the *spot check* in each session that they need to correctly rate the *golden images* in a proper range (*expert-set* rating ± 1 for $> 70\%$ images). Otherwise, the subject will be rejected for the next session. Considering the large number of images, to reduce visual fatigue, there is a rest session with at least 15 minutes between two sessions. To summarize, it took participants nearly 2 hours to finish one session, and all experiments were completed within a week. Each participant was compensated \$16 for each session according to the current ethical standard [79].

Annotation Quality Assessment. The reliability of results is of great importance while many studies did not report this entry. In this paper, we follow Otani *et al.*’s [68] recommendation that uses the inter-annotator agreement (IAA) metric (Krippendorff’s α [26]) to assess the quality of scoring. As a result, Krippendorff’s α for technical quality, rationality, and naturalness ratings are 0.32, 0.33, and 0.37, respectively, indicating appropriate variations among annotators. Furthermore, we use SRCC as a criterion, calculating the correlation between each participant and MOSs, to judge whether an annotator is an outlier. We removed two participants with extremely low SRCC (0.1851 and 0.2839), resulting in an improvement on Krippendorff’s α of 0.07 (from 0.32 to 0.39), 0.05 (from 0.33 to 0.38), and 0.04 (from 0.37 to 0.41) for technical quality, rationality, and naturalness scores, respectively.

Mean Opinion Scores. The mean opinion scores (MOSs) for each perspective are obtained by averaging cleaned ratings from different subjects. The final score is ranging from



Figure 12. **Four extended examples in AGIN that *technical* and *rationality* perspectives exhibit different effects on naturalness.** The two images on the left have different levels of technical and rationality scores, whereas the two images on the right have similar levels of technical and rationality scores. We also report the main factors with the highest proportion from the subject’s selection for each perspective.

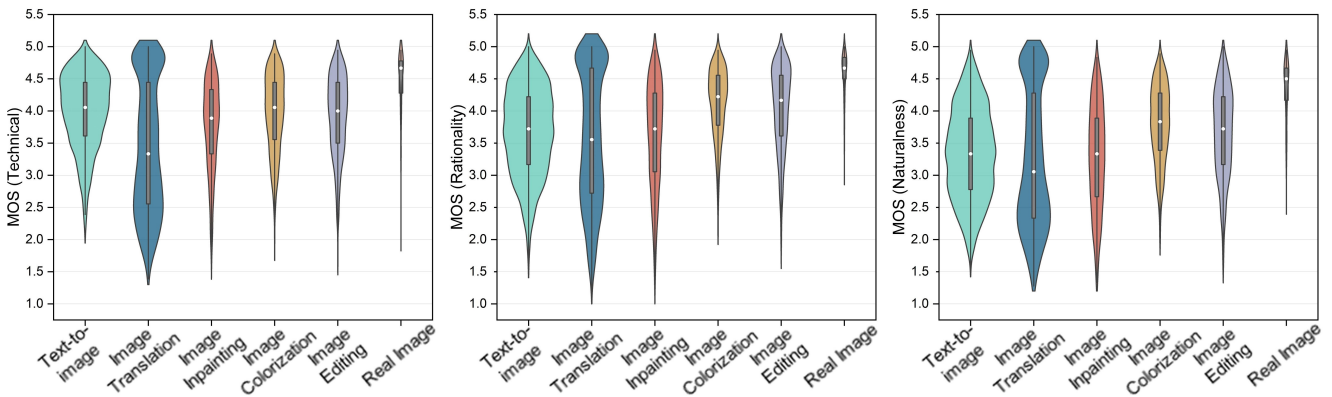


Figure 13. **Visualization of all categories in AGIN.** From left to right are the violin plots of technical quality, rationality, and overall naturalness scores. For each box, the white circle indicates the median and the edges of the box represent the 25th and 75th percentiles.

1 to 5. Specifically, the minimum and maximum score values of the MOS_T (technical perspective) are 1.39 and 5, and 1.17 and 5 for the MOS_R (rationality perspective), 1.28 and 5 for the overall naturalness.

Subjective Divergence between Perspectives. In Fig. 12, we further show four extended examples in AGIN, where the 1st image from left to right has worse *technical quality* (more *blurry*) while the 2nd image has significantly worse *rationality* score due to the relatively *nonexistent* contents. Such divergence (one has better technical quality, one has worse rationality) indicates that the overall naturalness scores not only depend on one aspect, which poses challenges to traditional IQA models supervised by a single MOS. Meanwhile, the 3rd and 4th images illustrate a more common scenario, possessing similar scores in terms of technical and rationality aspects.

A.3. Detailed Score Distribution

Detailed score distribution of different categories. As shown in Fig. 13, we visualize the detailed score distribution of different categories for all participants. It can be observed that the real images in AGIN have relatively high technical, rationality, and naturalness scores, which is consistent with our intention of controlling the quality of the rating results. Besides, AGIs from the image translation task have the widest distribution of scores for technical, rationality, and naturalness. In general, regardless of the number of images, all categories have a relatively balanced score distribution in terms of technical quality, rationality, and naturalness.

Detailed score distribution of different categories in terms of gender. We also visualize the detailed score distri-

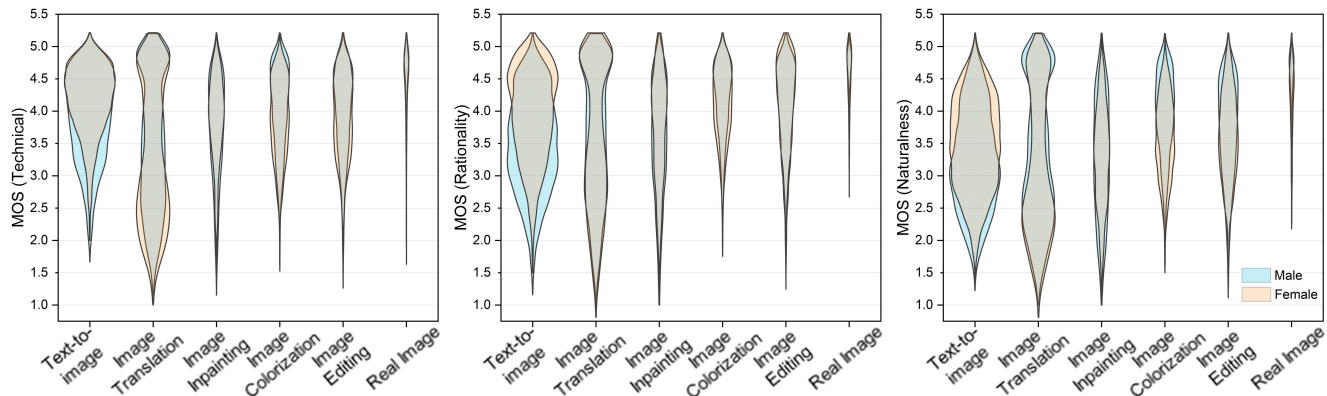


Figure 14. **Score distributions for male and female with different categories.** From left to right are the violin plots of technical quality, rationality, and overall naturalness scores.

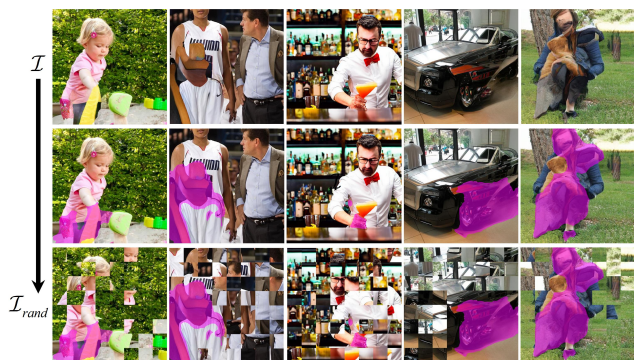


Figure 15. **Visualization of perceptual artifacts-guided patch partition.** The first row contains generated images from AGIN. The second row exhibits the prediction results of perceptual artifacts using the pre-trained model in [109]. In the last row, we show the resulted \mathcal{I}_{rand} after perceptual artifacts-guided patch partition.

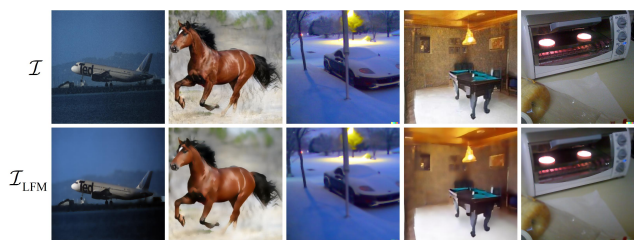


Figure 16. **Comparison of the original image and its corresponding low-frequency map from the AGIN database.** Zoom-in for better visualization.

bution of different categories for males and females in Fig. 14. We can observe that the score distribution of different categories for males and females is basically consistent except for the category of *text-to-image*. We speculate that people may have cognitive differences for familiar or unfamiliar objects.

B. Detailed Structure of the JOINT

In this section, we introduce some definitions and necessary notations that will be used in JOINT. Examples of the perceptual artifacts-guided patch partition in the technical prior branch are illustrated in Fig. 15.

B.1. Low-Frequency Map

To maintain the principal semantic information of the image while better reducing the impact of partial technical distortions, we utilize the piece-wise smooth image approximation algorithm [2] to generate the low-frequency map by minimizing:

$$\mathcal{F} = \frac{1}{2} \int_{\Omega} (\mathcal{I} - \mathcal{I}_{LFM})^2 dP + \mu \int_{\Omega \setminus E} |\nabla \mathcal{I}_{LFM}|^2 dP + \nu \int_E d\sigma, \quad (8)$$

where Ω and E denote the image domain and edge set, respectively. P indicates the pixel and $\int_E d\sigma$ represents the total edge length. The coefficients μ and ν are positive regularization constants. An example of low-frequency maps is shown in Fig. 16. We can observe that the LFM filters out some technical distortions but still preserves similar semantic information to the original image.

B.2. Definition of Wasserstein Distance

Given two multidimensional random variables P and Q with their distributions denoted as \mathcal{X} and \mathcal{Y} , respectively, the l -Wasserstein distance between them is defined as

$$W_l(P, Q) := \left(\inf_{\gamma \in \mathcal{J}(\mathcal{X}, \mathcal{Y})} \int \|p - q\|_l d\gamma(p, q) \right)^{1/l}, \quad (9)$$

where p and q are the masses of P and Q . $\gamma \in \mathcal{J}(\mathcal{X}, \mathcal{Y})$ is the joint distribution of (P, Q) . l is the order of the l -norm.

Additionally, for one-dimensional probability measures, the Eq. 9 is closed-form [10] and boils down to

$$W_l(P, Q) = \left(\int_0^1 |F_p^-(t) - F_q^-(t)|^p dt \right)^{1/l}, \quad (10)$$

where F_p^- represents the inverse cumulative function of P . t is the implicit variable that is used to integral $F_p^-(\cdot)$ and $F_q^-(\cdot)$ from 0 to 1.

B.3. Training Objective

Here, we discuss the concrete designs of the combination of the standard mean square error loss \mathcal{L}_{MSE} and Spearman Rank-order Correlation Coefficient (SRCC) loss $\mathcal{L}_{\text{SRCC}}$ as follows:

$$\mathcal{L}_{\text{MSE}} = \frac{1}{N} \sum_{n=1}^N \|y_n - \hat{y}_n\|_2^2, \quad (11)$$

$$\mathcal{L}_{\text{SRCC}} = 1 - \frac{\sum_n (v_n - \bar{v})(p_n - \bar{p})}{\sqrt{\sum_n (v_n - \bar{v})^2 \sum_n (p_n - \bar{p})^2}}, \quad (12)$$

$$\mathcal{L}_C = \mathcal{L}_{\text{MSE}} + \mathcal{L}_{\text{SRCC}}, \quad (13)$$

where the SRCC is defined in the form of the Pearson linear correlation coefficient (PLCC) between ranks [5, 46]. v_n and p_n denote the rank of the ground truth y_n and the rank of predicted score \hat{y}_n , respectively.

C. More Experimental Details

C.1. Implementation Details

We initialize all baselines using their own implementations and hyperparameters. In the rationality branch, all images are calculated at size 224×224 so as to satisfy the requirement of ResNet50. Besides, for penalty constraint \mathcal{L}_{WSD} , we set $l = 2$ as in [52], making the quality measure more sensitive to outliers. The N in \mathcal{L}_{WSD} is 5, corresponding to five stages in Resnet50 backbone. Before training, we randomly split the training, validation, and testing set into 7:1:2. There is no overlap of the same image content between each set. We repeat the split process 5 times and record the average performance as the final experimental results.

C.2. Evaluation Metrics

We adopt the widely used metrics in IQA literature [98]: Spearman rank-order correlation coefficient (SRCC) and Pearson linear correlation coefficient (PLCC), as our evaluation criteria. SRCC quantifies the extent to which the ranks of two variables are related, which ranges from -1 to 1. Given N distorted images, SRCC is computed as:

$$\text{SRCC} = 1 - \frac{6 \sum_{n=1}^N (v_n - p_n)^2}{N(N^2 - 1)}, \quad (14)$$

Predict better *Rationality* than *Technical*

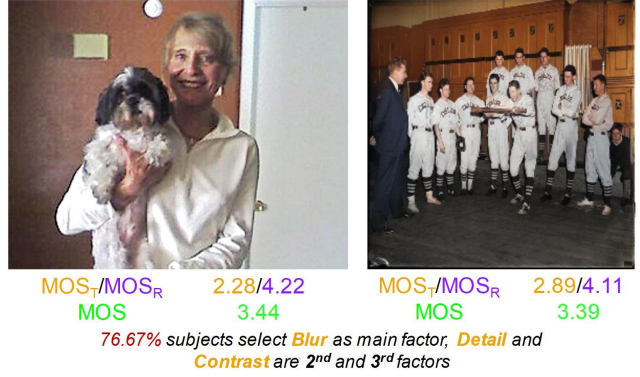


Figure 17. **Success case (I) of JOINT.** The images possess better rationality but worse technical quality (e.g., blur, detail, contrast).

Predict better *Rationality* than *Technical*

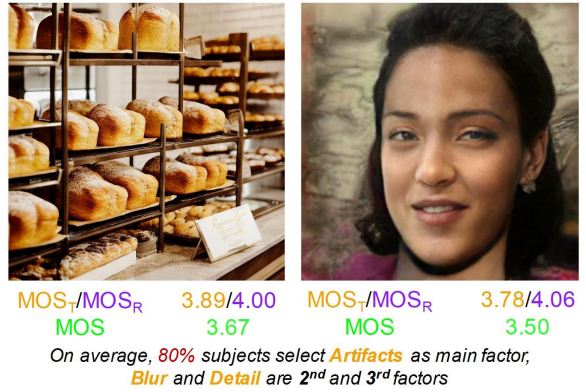


Figure 18. **Success case (II) of JOINT.** The images possess better rationality but worse technical quality (e.g., artifacts, blur, detail).

where v_n and p_n denote the rank of the ground truth y_n and the rank of predicted score \hat{y}_n , respectively. The higher the SRCC, the higher the monotonic correlation between ground truth and predicted score. Similarly, PLCC measures the linear correlation between predicted scores and ground truth scores, which can be formulated as:

$$\text{PLCC} = \frac{\sum_{n=1}^N (y_n - \bar{y})(\hat{y}_n - \bar{\hat{y}})}{\sqrt{\sum_{n=1}^N (y_n - \bar{y})^2} \sqrt{\sum_{n=1}^N (\hat{y}_n - \bar{\hat{y}})^2}}, \quad (15)$$

where \bar{y} and $\bar{\hat{y}}$ are the mean of ground truth and predicted score respectively.

C.3. Extended Qualitative Results

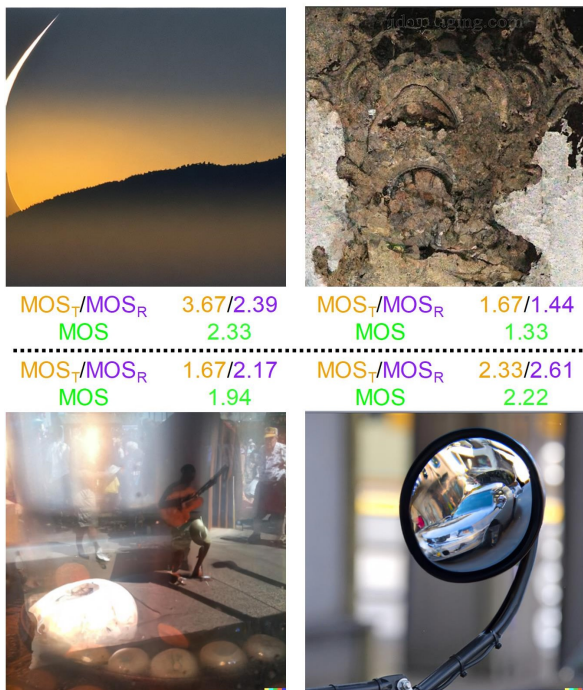
Success Cases. We visualized several successful cases (i.e., when the predicted results are consistent with subjective annotators in each dimension) for the proposed JOINT in Fig. 17, Fig. 18, and Fig. 19. Specifically, we can observe that our JOINT is sensitive to global technical distortions such

Predict better *Technical* than *Rationality*



Figure 19. **Success case (III) of JOINT.** The images possess better technical quality but worse rationality (e.g., existence, layout, context).

Predict better *Rationality* than *Technical*



Predict better *Technical* than *Rationality*

Figure 20. **Failure case of JOINT.** The images have better technical quality but worse rationality (e.g., existence, context, layout).

as blur, lack of detail, and contrast (Fig. 17). Moreover, the perceptual artifacts-guided patch partition strategy endows JOINT with the ability to measure the severity of local artifacts (Fig. 18). On the contrary, the rationality perceiving branch is not sensitive to technical distortion since we add deep feature regularization with filtered low-frequency information, and it is very sensitive to the rationality of con-

tents and can recognize the very unusual compositions and objects in images (Fig. 19). All these cases further demonstrate the effectiveness of the JOINT in jointly learning from both perspectives in image naturalness assessment.

Failure Cases. As for the failure cases, we notice that most of them are difficult to recognize (*poor sensory clarity*, the top one in Fig. 20) or are extremely blurry with a small part of clear areas (*mirror reflections*, the bottom one in Fig. 20). Such cases are more frequent in photography that photographers gain prominence over the target by blurring the background, yet the model can experience challenges in predicting technical quality and rationality, resulting in a failure in naturalness evaluation.

References

- [1] Mirko Agarla, Luigi Celona, Raimondo Schettini, and Claudio Rota. Quality assessment of enhanced videos guided by aesthetics and technical quality attributes. In *Proceedings of the IEEE/CVF Conference on Computer Vision and Pattern Recognition*, pages 1533–1541, 2023. 5
- [2] Leah Bar, N. Sochen, and N. Kiryati. Semi-blind image restoration via mumford-shah regularization. *IEEE Transactions on Image Processing*, 15:483–493, 2006. 6, 14
- [3] Ayman Beghdadi, Malik Mallem, and Lotfi Beji. Benchmarking performance of object detection under image distortions in an uncontrolled environment. In *2022 IEEE International Conference on Image Processing (ICIP)*, pages 2071–2075. IEEE, 2022. 3
- [4] Mikołaj Bińkowski, Danica J Sutherland, Michael Arbel, and Arthur Gretton. Demystifying mmd gans. *arXiv preprint arXiv:1801.01401*, 2018. 2
- [5] Mathieu Blondel, Olivier Teboul, Quentin Berthet, and Josip Djolonga. Fast differentiable sorting and ranking. In *International Conference on Machine Learning*, pages 950–959. PMLR, 2020. 15
- [6] Tim Brooks, Aleksander Holynski, and Alexei A Efros. Instructpix2pix: Learning to follow image editing instructions. In *Proceedings of the IEEE/CVF Conference on Computer Vision and Pattern Recognition*, pages 18392–18402, 2023. 1, 2, 9, 11
- [7] RIR BT. Methodology for the subjective assessment of the quality of television pictures. *International Telecommunication Union*, 4, 2002. 12
- [8] M Cadfk and Pavel Slavík. The naturalness of reproduced high dynamic range images. In *Ninth International Conference on Information Visualisation (IV'05)*, pages 920–925. IEEE, 2005. 1, 3

- [9] Yihan Cao, Siyu Li, Yixin Liu, Zhiling Yan, Yutong Dai, Philip S Yu, and Lichao Sun. A comprehensive survey of ai-generated content (aigc): A history of generative ai from gan to chatgpt. *arXiv preprint arXiv:2303.04226*, 2023. **1**
- [10] Elsa Cazelles, Arnaud Robert, and Felipe Tobar. The wasserstein-fourier distance for stationary time series. *IEEE Transactions on Signal Processing*, 69:709–721, 2020. **6, 15**
- [11] Yixiong Chen. X-iqe: explainable image quality evaluation for text-to-image generation with visual large language models. *arXiv preprint arXiv:2305.10843*, 2023. **3**
- [12] Yunzhuo Chen, Naveed Akhtar, Nur Al Hasan Haldar, and Ajmal Mian. On quantifying and improving realism of images generated with diffusion. *arXiv preprint arXiv:2309.14756*, 2023. **2**
- [13] Yang Chen, Yu-Kun Lai, and Yong-Jin Liu. Cartoon-gan: Generative adversarial networks for photo cartoonization. In *Proceedings of the IEEE conference on computer vision and pattern recognition*, pages 9465–9474, 2018. **9, 11**
- [14] Seo Young Choi, M Luo, Michael Pointer, and Peter Rhodes. Investigation of large display color image appearance—iii: Modeling image naturalness. *Journal of Imaging Science and Technology*, 53(3):31104–1, 2009. **1, 3**
- [15] Alexandre Ciancio, Eduardo AB da Silva, Amir Said, Ramin Samadani, Pere Obrador, et al. No-reference blur assessment of digital pictures based on multi-feature classifiers. *IEEE Transactions on image processing*, 20(1):64–75, 2010. **7**
- [16] Marco Cristani, Alessandro Vinciarelli, Cristina Segalin, and Alessandro Perina. Unveiling the multimedia unconscious: Implicit cognitive processes and multimedia content analysis. In *Proceedings of the 21st ACM international conference on Multimedia*, pages 213–222, 2013. **7**
- [17] Huib de Ridder. Naturalness and image quality: saturation and lightness variation in color images of natural scenes. *Journal of imaging science and technology*, 40(6):487–493, 1996. **3**
- [18] Huib de Ridder, Frans JJ Blommaert, and Elena A Fedorovskaya. Naturalness and image quality: chroma and hue variation in color images of natural scenes. In *Human Vision, Visual Processing, and Digital Display VI*, volume 2411, pages 51–61. SPIE, 1995. **1, 3**
- [19] Dreamlike.art. <https://dreamlike.art>. 2023. **1, 9, 11**
- [20] Yuming Fang, Hanwei Zhu, Yan Zeng, Kede Ma, and Zhou Wang. Perceptual quality assessment of smartphone photography. In *Proceedings of the IEEE/CVF Conference on Computer Vision and Pattern Recognition*, pages 3677–3686, 2020. **7**
- [21] Deepti Ghadiyaram and Alan C Bovik. Massive online crowdsourced study of subjective and objective picture quality. *IEEE Transactions on Image Processing*, 25(1):372–387, 2015. **7, 9**
- [22] Melvyn A Goodale and A David Milner. Separate visual pathways for perception and action. *Trends in neurosciences*, 15(1):20–25, 1992. **5**
- [23] Jinjin Gu, Haoming Cai, Chao Dong, Jimmy S Ren, Radu Timofte, Yuan Gong, Shanshan Lao, Shuwei Shi, Jiahao Wang, Sidi Yang, et al. Ntire 2022 challenge on perceptual image quality assessment. In *Proceedings of the IEEE/CVF Conference on Computer Vision and Pattern Recognition*, pages 951–967, 2022. **7**
- [24] Ke Gu, Shiqi Wang, Guangtao Zhai, Siwei Ma, Xiaokang Yang, Weisi Lin, Wenjun Zhang, and Wen Gao. Blind quality assessment of tone-mapped images via analysis of information, naturalness, and structure. *IEEE Transactions on Multimedia*, 18(3):432–443, 2016. **1, 2, 3**
- [25] Pengfei Guo, Lang He, Shuangyin Liu, Delu Zeng, and Hantao Liu. Underwater image quality assessment: Subjective and objective methods. *IEEE Transactions on Multimedia*, 24:1980–1989, 2021. **2**
- [26] Andrew F Hayes and Klaus Krippendorff. Answering the call for a standard reliability measure for coding data. *Communication methods and measures*, 1(1):77–89, 2007. **12**
- [27] Kaiming He, Xiangyu Zhang, Shaoqing Ren, and Jian Sun. Deep residual learning for image recognition. In *Proceedings of the IEEE conference on computer vision and pattern recognition*, pages 770–778, 2016. **7**
- [28] Shuai He, Anlong Ming, Yaqi Li, Jinyuan Sun, ShunTian Zheng, and Huadong Ma. Thinking image color aesthetics assessment: Models, datasets and benchmarks. In *Proceedings of the IEEE/CVF International Conference on Computer Vision*, pages 21838–21847, 2023. **5, 7, 8**
- [29] Shuai He, Yongchang Zhang, Rui Xie, Dongxiang Jiang, and Anlong Ming. Rethinking image aesthetics assessment: Models, datasets and benchmarks. In *Proceedings of the Thirty-First International Joint Conference on Artificial Intelligence, IJCAI-22*, pages 942–948, 2022. **5, 7, 8**
- [30] Jack Hessel, Ari Holtzman, Maxwell Forbes, Ronan Le Bras, and Yejin Choi. Clipscore: A reference-

- free evaluation metric for image captioning. *arXiv preprint arXiv:2104.08718*, 2021. 3
- [31] Martin Heusel, Hubert Ramsauer, Thomas Unterthiner, Bernhard Nessler, and Sepp Hochreiter. Gans trained by a two time-scale update rule converge to a local nash equilibrium. *Advances in neural information processing systems*, 30, 2017. 2
- [32] Vlad Hosu, Hanhe Lin, Tamas Sziranyi, and Dietmar Saupe. Koniq-10k: An ecologically valid database for deep learning of blind image quality assessment. *IEEE Transactions on Image Processing*, 29:4041–4056, 2020. 7, 9
- [33] David Ingle. Two visual systems in the frog. *Science*, 181(4104):1053–1055, 1973. 5
- [34] Chang Jiang, Fei Gao, Biao Ma, Yuhao Lin, Nannan Wang, and Gang Xu. Masked and adaptive transformer for exemplar based image translation. In *Proceedings of the IEEE/CVF Conference on Computer Vision and Pattern Recognition*, pages 22418–22427, 2023. 1, 9, 11
- [35] Xiaoyang Kang, Tao Yang, Wenqi Ouyang, Peiran Ren, Lingzhi Li, and Xuansong Xie. Ddcolor: Towards photo-realistic and semantic-aware image colorization via dual decoders. *arXiv preprint arXiv:2212.11613*, 2022. 1, 9, 11
- [36] Tero Karras, Samuli Laine, and Timo Aila. A style-based generator architecture for generative adversarial networks. In *Proceedings of the IEEE/CVF conference on computer vision and pattern recognition*, pages 4401–4410, 2019. 9, 11
- [37] Tero Karras, Samuli Laine, Miika Aittala, Janne Hellsten, Jaakko Lehtinen, and Timo Aila. Analyzing and improving the image quality of stylegan. In *Proceedings of the IEEE/CVF conference on computer vision and pattern recognition*, pages 8110–8119, 2020. 11
- [38] Junjie Ke, Qifei Wang, Yilin Wang, Peyman Milanfar, and Feng Yang. Musiq: Multi-scale image quality transformer. In *Proceedings of the IEEE/CVF International Conference on Computer Vision*, pages 5148–5157, 2021. 7, 8
- [39] Diederik P Kingma and Jimmy Ba. Adam: A method for stochastic optimization. *arXiv preprint arXiv:1412.6980*, 2014. 7
- [40] Yuval Kirstain, Adam Polyak, Uriel Singer, Shahbuland Matiana, Joe Penna, and Omer Levy. Pick-a-pic: An open dataset of user preferences for text-to-image generation. *arXiv preprint arXiv:2305.01569*, 2023. 3
- [41] Gihyun Kwon and Jong Chul Ye. Diffusion-based image translation using disentangled style and content representation. In *ICLR*, 2023. 1, 2, 9, 11
- [42] Tuomas Kynkäänniemi, Tero Karras, Samuli Laine, Jaakko Lehtinen, and Timo Aila. Improved precision and recall metric for assessing generative models. *Advances in Neural Information Processing Systems*, 32, 2019. 2
- [43] Eric C Larson and Damon M Chandler. Most apparent distortion: full-reference image quality assessment and the role of strategy. *Journal of electronic imaging*, 19(1):011006–011006, 2010. 7, 9
- [44] Quyet-Tien Le, Patricia Ladret, Huu-Tuan Nguyen, and Alice Caplier. Study of naturalness in tone-mapped images. *Computer Vision and Image Understanding*, 196:102971, 2020. 1, 3
- [45] Bin Li, Yi Lu, Wei Pang, and Huixin Xu. Image colorization using cyclegan with semantic and spatial rationality. *Multimedia Tools and Applications*, pages 1–15, 2023. 1
- [46] Bowen Li, Weixia Zhang, Meng Tian, Guangtao Zhai, and Xianpei Wang. Blindly assess quality of in-the-wild videos via quality-aware pre-training and motion perception. *IEEE Transactions on Circuits and Systems for Video Technology*, 32(9):5944–5958, 2022. 6, 15
- [47] Chunyi Li, Zicheng Zhang, Haoning Wu, Wei Sun, Xiongkuo Min, Xiaohong Liu, Guangtao Zhai, and Weisi Lin. Agiqa-3k: An open database for ai-generated image quality assessment. *IEEE Transactions on Circuits and Systems for Video Technology*, 2023. 3
- [48] Dingquan Li, Tingting Jiang, and Ming Jiang. Norm-in-norm loss with faster convergence and better performance for image quality assessment. In *Proceedings of the 28th ACM International Conference on Multimedia*, pages 789–797, 2020. 6
- [49] Leida Li, Hancheng Zhu, Sicheng Zhao, Guiguang Ding, and Weisi Lin. Personality-assisted multi-task learning for generic and personalized image aesthetics assessment. *IEEE Transactions on Image Processing*, 29:3898–3910, 2020. 5, 7, 8
- [50] Simin Li, Shuning Zhang, Gujun Chen, Dong Wang, Pu Feng, Jiakai Wang, Aishan Liu, Xin Yi, and Xianglong Liu. Towards benchmarking and assessing visual naturalness of physical world adversarial attacks. In *Proceedings of the IEEE/CVF Conference on Computer Vision and Pattern Recognition*, pages 12324–12333, 2023. 2, 9
- [51] Wenbo Li, Zhe Lin, Kun Zhou, Lu Qi, Yi Wang, and Jiaya Jia. Mat: Mask-aware transformer for

- large hole image inpainting. In *Proceedings of the IEEE/CVF conference on computer vision and pattern recognition*, pages 10758–10768, 2022. 1, 9, 11
- [52] Xigran Liao, Baoliang Chen, Hanwei Zhu, Shiqi Wang, Mingliang Zhou, and Sam Kwong. Deep-wsd: Projecting degradations in perceptual space to wasserstein distance in deep feature space. *Proceedings of the 30th ACM International Conference on Multimedia*, 2022. 6, 15
- [53] Hanhe Lin, Vlad Hosu, and Dietmar Saupe. Kadid-10k: A large-scale artificially distorted iqa database. In *2019 Eleventh International Conference on Quality of Multimedia Experience (QoMEX)*, pages 1–3. IEEE, 2019. 7, 9
- [54] Tsung-Yi Lin, Michael Maire, Serge Belongie, James Hays, Pietro Perona, Deva Ramanan, Piotr Dollár, and C Lawrence Zitnick. Microsoft coco: Common objects in context. In *Computer Vision—ECCV 2014: 13th European Conference, Zurich, Switzerland, September 6–12, 2014, Proceedings, Part V 13*, pages 740–755. Springer, 2014. 9, 11
- [55] Yutao Liu, Ke Gu, Yongbing Zhang, Xiu Li, Guangtao Zhai, Debin Zhao, and Wen Gao. Unsupervised blind image quality evaluation via statistical measurements of structure, naturalness, and perception. *IEEE Transactions on Circuits and Systems for Video Technology*, 30(4):929–943, 2019. 2
- [56] Ze Liu, Yutong Lin, Yue Cao, Han Hu, Yixuan Wei, Zheng Zhang, Stephen Lin, and Baining Guo. Swin transformer: Hierarchical vision transformer using shifted windows. In *Proceedings of the IEEE/CVF international conference on computer vision*, pages 10012–10022, 2021. 7
- [57] Ziwei Liu, Ping Luo, Shi Qiu, Xiaogang Wang, and Xiaoou Tang. Deepfashion: Powering robust clothes recognition and retrieval with rich annotations. In *Proceedings of the IEEE conference on computer vision and pattern recognition*, pages 1096–1104, 2016. 9, 11
- [58] Ziwei Liu, Ping Luo, Xiaogang Wang, and Xiaoou Tang. Deep learning face attributes in the wild. In *Proceedings of the IEEE international conference on computer vision*, pages 3730–3738, 2015. 9, 11
- [59] Zeyu Lu, Di Huang, Lei Bai, Xihui Liu, Jingjing Qu, and Wanli Ouyang. Seeing is not always believing: A quantitative study on human perception of ai-generated images. *arXiv preprint arXiv:2304.13023*, 2023. 1, 3
- [60] Andreas Lugmayr, Martin Danelljan, Andres Romero, Fisher Yu, Radu Timofte, and Luc Van Gool. Repaint: Inpainting using denoising diffusion probabilistic models. In *Proceedings of the IEEE/CVF Conference on Computer Vision and Pattern Recognition*, pages 11461–11471, 2022. 1, 2, 9, 11
- [61] Kede Ma, Zhengfang Duanmu, Qingbo Wu, Zhou Wang, Hongwei Yong, Hongliang Li, and Lei Zhang. Waterloo exploration database: New challenges for image quality assessment models. *IEEE Transactions on Image Processing*, 26(2):1004–1016, 2016. 9
- [62] Midjourney. <https://www.midjourney.com>. 2023. 1, 2, 9, 11
- [63] Anish Mittal, Anush Krishna Moorthy, and Alan Conrad Bovik. No-reference image quality assessment in the spatial domain. *IEEE Transactions on image processing*, 21(12):4695–4708, 2012. 7, 8
- [64] Anish Mittal, Rajiv Soundararajan, and Alan C Bovik. Making a “completely blind” image quality analyzer. *IEEE Signal processing letters*, 20(3):209–212, 2013. 7, 8
- [65] Naila Murray, Luca Marchesotti, and Florent Perronnin. Ava: A large-scale database for aesthetic visual analysis. In *2012 IEEE conference on computer vision and pattern recognition*, pages 2408–2415. IEEE, 2012. 7
- [66] Alex Nichol, Prafulla Dhariwal, Aditya Ramesh, Pranav Shyam, Pamela Mishkin, Bob McGrew, Ilya Sutskever, and Mark Chen. Glide: Towards photorealistic image generation and editing with text-guided diffusion models. *arXiv preprint arXiv:2112.10741*, 2021. 1, 2
- [67] Joel Norman. Two visual systems and two theories of perception: An attempt to reconcile the constructivist and ecological approaches. *Behavioral and brain sciences*, 25(1):73–96, 2002. 5
- [68] Mayu Otani, Riku Togashi, Yu Sawai, Ryosuke Ishigami, Yuta Nakashima, Esa Rahtu, Janne Heikkilä, and Shin’ichi Satoh. Toward verifiable and reproducible human evaluation for text-to-image generation. In *Proceedings of the IEEE/CVF Conference on Computer Vision and Pattern Recognition*, pages 14277–14286, 2023. 2, 3, 12
- [69] Xingang Pan, Ayush Tewari, Thomas Leimkühler, Lingjie Liu, Abhimitra Meka, and Christian Theobalt. Drag your gan: Interactive point-based manipulation on the generative image manifold. In *ACM SIGGRAPH 2023 Conference Proceedings*, pages 1–11, 2023. 1, 9, 11
- [70] Or Patashnik, Zongze Wu, Eli Shechtman, Daniel Cohen-Or, and Dani Lischinski. Styleclip: Text-driven manipulation of stylegan imagery. In *Proceed-*

- ings of the *IEEE/CVF International Conference on Computer Vision*, pages 2085–2094, 2021. 1, 2, 9, 11
- [71] Nikolay Ponomarenko, Lina Jin, Oleg Ieremeiev, Vladimir Lukin, Karen Egiazarian, Jaakko Astola, Benoit Vozel, Kacem Chehdi, Marco Carli, Federica Battisti, et al. Image database tid2013: Peculiarities, results and perspectives. *Signal processing: Image communication*, 30:57–77, 2015. 7, 9
- [72] Nikolay Ponomarenko, Vladimir Lukin, Alexander Zelensky, Karen Egiazarian, Marco Carli, and Federica Battisti. Tid2008-a database for evaluation of full-reference visual quality assessment metrics. *Advances of modern radioelectronics*, 10(4):30–45, 2009. 9
- [73] Aditya Ramesh, Prafulla Dhariwal, Alex Nichol, Casey Chu, and Mark Chen. Hierarchical text-conditional image generation with clip latents. *arXiv preprint arXiv:2204.06125*, 1(2):3, 2022. 1, 2
- [74] Robin Rombach, Andreas Blattmann, Dominik Lorenz, Patrick Esser, and Björn Ommer. High-resolution image synthesis with latent diffusion models. In *Proceedings of the IEEE/CVF conference on computer vision and pattern recognition*, pages 10684–10695, 2022. 1, 2, 9, 11
- [75] Olga Russakovsky, Jia Deng, Hao Su, Jonathan Krause, Sanjeev Satheesh, Sean Ma, Zhiheng Huang, Andrej Karpathy, Aditya Khosla, Michael Bernstein, et al. Imagenet large scale visual recognition challenge. *International journal of computer vision*, 115:211–252, 2015. 7, 9, 11
- [76] Chitwan Saharia, William Chan, Saurabh Saxena, Lala Li, Jay Whang, Emily L Denton, Kamyar Ghasemipour, Raphael Gontijo Lopes, Burcu Karagol Ayan, Tim Salimans, et al. Photorealistic text-to-image diffusion models with deep language understanding. *Advances in Neural Information Processing Systems*, 35:36479–36494, 2022. 1, 2, 9, 11
- [77] Tim Salimans, Ian Goodfellow, Wojciech Zaremba, Vicki Cheung, Alec Radford, and Xi Chen. Improved techniques for training gans. *Advances in neural information processing systems*, 29, 2016. 2
- [78] H Sheikh. Live image quality assessment database release 2. <http://live.ece.utexas.edu/research/quality>, 2005. 7, 9
- [79] M Six Silberman, Bill Tomlinson, Rochelle LaPlante, Joel Ross, Lilly Irani, and Andrew Zaldivar. Responsible research with crowds: pay crowdworkers at least minimum wage. *Communications of the ACM*, 61(3):39–41, 2018. 12
- [80] Shaolin Su, Qingsen Yan, Yu Zhu, Cheng Zhang, Xin Ge, Jinqiu Sun, and Yanning Zhang. Blindly assess image quality in the wild guided by a self-adaptive hyper network. In *Proceedings of the IEEE/CVF Conference on Computer Vision and Pattern Recognition*, pages 3667–3676, 2020. 7, 8
- [81] Wei Sun, Xiongkuo Min, Danyang Tu, Siwei Ma, and Guangtao Zhai. Blind quality assessment for in-the-wild images via hierarchical feature fusion and iterative mixed database training. *IEEE Journal of Selected Topics in Signal Processing*, 2023. 5
- [82] Wen Sun, Fei Zhou, and Qingmin Liao. Mdid: A multiply distorted image database for image quality assessment. *Pattern Recognition*, 61:153–168, 2017. 9
- [83] Hanzhang Wang, Deming Zhai, Xianming Liu, Junjun Jiang, and Wen Gao. Unsupervised deep exemplar colorization via pyramid dual non-local attention. *IEEE Transactions on Image Processing*, 32:4114–4127, 2023. 1, 9, 11
- [84] Jianyi Wang, Kelvin CK Chan, and Chen Change Loy. Exploring clip for assessing the look and feel of images. In *Proceedings of the AAAI Conference on Artificial Intelligence*, volume 37, pages 2555–2563, 2023. 7
- [85] Jiarui Wang, Huiyu Duan, Jing Liu, Shi Chen, Xiongkuo Min, and Guangtao Zhai. Aigciqa2023: A large-scale image quality assessment database for ai generated images: from the perspectives of quality, authenticity and correspondence. *arXiv preprint arXiv:2307.00211*, 2023. 3
- [86] Sheng-Yu Wang, Oliver Wang, Andrew Owens, Richard Zhang, and Alexei A Efros. Detecting photoshopped faces by scripting photoshop. In *Proceedings of the IEEE/CVF International Conference on Computer Vision*, pages 10072–10081, 2019. 5
- [87] Haoning Wu, Chaofeng Chen, Jingwen Hou, Liang Liao, Annan Wang, Wenxiu Sun, Qiong Yan, and Weisi Lin. Fast-vqa: Efficient end-to-end video quality assessment with fragment sampling. In *European Conference on Computer Vision*, pages 538–554. Springer, 2022. 5
- [88] Haoning Wu, Erli Zhang, Liang Liao, Chaofeng Chen, Jingwen Hou, Annan Wang, Wenxiu Sun, Qiong Yan, and Weisi Lin. Exploring video quality assessment on user generated contents from aesthetic and technical perspectives. In *Proceedings of the IEEE/CVF International Conference on Computer Vision*, pages 20144–20154, 2023. 5, 6
- [89] Haoning Wu, Erli Zhang, Liang Liao, Chaofeng Chen, Jingwen Hou, Annan Wang, Wenxiu Sun,

- Qiong Yan, and Weisi Lin. Towards explainable in-the-wild video quality assessment: a database and a language-prompted approach. *arXiv preprint arXiv:2305.12726*, 2023. 3, 5
- [90] Haoning Wu, Zicheng Zhang, Erli Zhang, Chaofeng Chen, Liang Liao, Annan Wang, Kaixin Xu, Chunyi Li, Jingwen Hou, Guangtao Zhai, et al. Q-instruct: Improving low-level visual abilities for multi-modality foundation models. *arXiv preprint arXiv:2311.06783*, 2023. 7
- [91] Jiayang Wu, Wensheng Gan, Zefeng Chen, Shicheng Wan, and Hong Lin. Ai-generated content (aigc): A survey. *arXiv preprint arXiv:2304.06632*, 2023. 1, 2
- [92] Menghan Xia, Wenbo Hu, Tien-Tsin Wong, and Jue Wang. Disentangled image colorization via global anchors. *ACM Transactions on Graphics (TOG)*, 41(6):1–13, 2022. 1, 2, 9, 11
- [93] Bo Yan, Bahetiyaer Bare, and Weimin Tan. Naturalness-aware deep no-reference image quality assessment. *IEEE Transactions on Multimedia*, 21(10):2603–2615, 2019. 1, 2, 3
- [94] Sidi Yang, Tianhe Wu, Shuwei Shi, Shanshan Lao, Yuan Gong, Mingdeng Cao, Jiahao Wang, and Yujia Yang. Maniqa: Multi-dimension attention network for no-reference image quality assessment. In *Proceedings of the IEEE/CVF Conference on Computer Vision and Pattern Recognition*, pages 1191–1200, 2022. 7, 8
- [95] Ran Yi, Haoyuan Tian, Zhihao Gu, Yu-Kun Lai, and Paul L Rosin. Towards artistic image aesthetics assessment: a large-scale dataset and a new method. In *Proceedings of the IEEE/CVF Conference on Computer Vision and Pattern Recognition*, pages 22388–22397, 2023. 5, 7, 8
- [96] Zhenqiang Ying, Haoran Niu, Praful Gupta, Dhruv Mahajan, Deepti Ghadiyaram, and Alan Bovik. From patches to pictures (paq-2-piq): Mapping the perceptual space of picture quality. In *Proceedings of the IEEE/CVF Conference on Computer Vision and Pattern Recognition*, pages 3575–3585, 2020. 7
- [97] Xiangxu Yu, Christos G Bampis, Praful Gupta, and Alan Conrad Bovik. Predicting the quality of images compressed after distortion in two steps. *IEEE Transactions on Image Processing*, 28(12):5757–5770, 2019. 3
- [98] Guangtao Zhai and Xiongkuo Min. Perceptual image quality assessment: a survey. *Science China Information Sciences*, 63:1–52, 2020. 15
- [99] Fangneng Zhan, Yingchen Yu, Rongliang Wu, Jiahui Zhang, Kaiwen Cui, Aoran Xiao, Shijian Lu, and Chunyan Miao. Bi-level feature alignment for versatile image translation and manipulation. In *European Conference on Computer Vision*, pages 224–241. Springer, 2022. 1, 2, 9, 11
- [100] Kai Zhang, Lingbo Mo, Wenhui Chen, Huan Sun, and Yu Su. Magicbrush: A manually annotated dataset for instruction-guided image editing. *arXiv preprint arXiv:2306.10012*, 2023. 1, 9, 11
- [101] Lvmin Zhang and Maneesh Agrawala. Adding conditional control to text-to-image diffusion models. *arXiv preprint arXiv:2302.05543*, 2023. 2
- [102] Lingzhi Zhang, Yuqian Zhou, Connelly Barnes, Sohrab Amirghodsi, Zhe Lin, Eli Shechtman, and Jianbo Shi. Perceptual artifacts localization for inpainting. In *European Conference on Computer Vision*, pages 146–164. Springer, 2022. 5
- [103] Pan Zhang, Xiaoyi Dong Bin Wang, Yuhang Cao, Chao Xu, Linke Ouyang, Zhiyuan Zhao, Shuangrui Ding, Songyang Zhang, Haodong Duan, Hang Yan, et al. Internlm-xcomposer: A vision-language large model for advanced text-image comprehension and composition. *arXiv preprint arXiv:2309.15112*, 2023. 7
- [104] Pan Zhang, Bo Zhang, Dong Chen, Lu Yuan, and Fang Wen. Cross-domain correspondence learning for exemplar-based image translation. In *Proceedings of the IEEE/CVF Conference on Computer Vision and Pattern Recognition*, pages 5143–5153, 2020. 1, 2, 9, 11
- [105] Richard Zhang, Phillip Isola, Alexei A Efros, Eli Shechtman, and Oliver Wang. The unreasonable effectiveness of deep features as a perceptual metric. In *Proceedings of the IEEE conference on computer vision and pattern recognition*, pages 586–595, 2018. 6
- [106] Weixia Zhang, Kede Ma, Jia Yan, Dexiang Deng, and Zhou Wang. Blind image quality assessment using a deep bilinear convolutional neural network. *IEEE Transactions on Circuits and Systems for Video Technology*, 30(1):36–47, 2018. 7, 8
- [107] Weixia Zhang, Kede Ma, Guangtao Zhai, and Xiaokang Yang. Uncertainty-aware blind image quality assessment in the laboratory and wild. *IEEE Transactions on Image Processing*, 30:3474–3486, 2021. 7, 8
- [108] Weixia Zhang, Guangtao Zhai, Ying Wei, Xiaokang Yang, and Kede Ma. Blind image quality assessment via vision-language correspondence: A multitask learning perspective. In *Proceedings of the IEEE/CVF Conference on Computer Vision and Pattern Recognition*, pages 14071–14081, 2023. 7

- [109] Zicheng Zhang, Chunyi Li, Wei Sun, Xiaohong Liu, Xionghuo Min, and Guangtao Zhai. A perceptual quality assessment exploration for aigc images. *arXiv preprint arXiv:2303.12618*, 2023. [2](#), [3](#), [5](#), [14](#)
- [110] Lilei Zheng, Ying Zhang, and Vrizlynn LL Thing. A survey on image tampering and its detection in real-world photos. *Journal of Visual Communication and Image Representation*, 58:380–399, 2019. [5](#)
- [111] Yannan Zheng, Weiling Chen, Rongfu Lin, Tiesong Zhao, and Patrick Le Callet. Uif: An objective quality assessment for underwater image enhancement. *IEEE Transactions on Image Processing*, 31:5456–5468, 2022. [2](#)
- [112] Bolei Zhou, Agata Lapedriza, Aditya Khosla, Aude Oliva, and Antonio Torralba. Places: A 10 million image database for scene recognition. *IEEE transactions on pattern analysis and machine intelligence*, 40(6):1452–1464, 2017. [9](#), [11](#)
- [113] Bolei Zhou, Hang Zhao, Xavier Puig, Sanja Fidler, Adela Barriuso, and Antonio Torralba. Scene parsing through ade20k dataset. In *Proceedings of the IEEE conference on computer vision and pattern recognition*, pages 633–641, 2017. [9](#), [11](#)
- [114] Mingjian Zhu, Hanting Chen, Qiangyu Yan, Xudong Huang, Guanyu Lin, Wei Li, Zhijun Tu, Hailin Hu, Jie Hu, and Yunhe Wang. Genimage: A million-scale benchmark for detecting ai-generated image. *arXiv preprint arXiv:2306.08571*, 2023. [3](#)